AEDC-TR-85-43

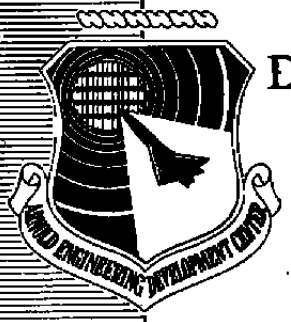

Development of a Two-Dimensional/Axisymmetric Implicit Navier-Stokes Solver Using Flux-Difference Splitting Concepts and Fully General Geometry

Richard G. Hindman
The University of Texas at Arlington

(Revised, October 1985)

Final Report for Period March 1, 1984 — February 28, 1985

Approved for public release; distribution unlimited.

ARNOLD ENGINEERING DEVELOPMENT CENTER
ARNOLD AIR FORCE STATION, TENNESSEE
AIR FORCE SYSTEMS COMMAND
UNITED STATES AIR FORCE

NOTICES

When U. S. Government drawings, specifications, or other data are used for any purpose other than a definitely related Government procurement operation, the Government thereby incurs no responsibility nor any obligation whatsoever, and the fact that the government may have formulated, furnished, or in any way supplied the said drawings, specifications, or other data, is not to be regarded by implication or otherwise, or in any manner licensing the holder or any other person or corporation, or conveying any rights or permission to manufacture, use, or sell any patented invention that may in any way be related thereto.

Qualified users may obtain copies of this report from the Defense Technical Information Center.

References to named commercial products in this report are not to be considered in any sense as an endorsement of the product by the United States Air Force or the Government.

This report has been reviewed by the Office of Public Affairs (PA) and is releasable to the National Technical Information Service (NTIS). At NTIS, it will be available to the general public, including foreign nations.

APPROVAL STATEMENT

This report has been reviewed and approved.

Keith L Kushman

KEITH L. KUSHMAN
Directorate of Technology
Deputy for Operations

Approved for publication:

FOR THE COMMANDER

Marion L. Laster

MARION L. LASTER
Director of Technology
Deputy for Operations

UNCLASSIFIED
SECURITY CLASSIFICATION OF THIS PAGE

REPORT DOCUMENTATION PAGE

1a. REPORT SECURITY CLASSIFICATION UNCLASSIFIED	1b. RESTRICTIVE MARKINGS
2a. SECURITY CLASSIFICATION AUTHORITY	3. DISTRIBUTION/AVAILABILITY OF REPORT Approved for public release; distribution unlimited.
2b. DECLASSIFICATION/DOWNGRADING SCHEDULE	
4. PERFORMING ORGANIZATION REPORT NUMBER(S) AEDC-TR-85-43	5. MONITORING ORGANIZATION REPORT NUMBER(S)
6a. NAME OF PERFORMING ORGANIZATION Arnold Engineering Development Center 6b. OFFICE SYMBOL (If applicable) DO	7a. NAME OF MONITORING ORGANIZATION
6c. ADDRESS (City, State and ZIP Code) Air Force Systems Command Arnold Air Force Station, TN 37389-5000	7b. ADDRESS (City, State and ZIP Code)
8a. NAME OF FUNDING/SPONSORING ORGANIZATION Arnold Engineering Development Center 8b. OFFICE SYMBOL (If applicable) DOT	9. PROCUREMENT INSTRUMENT IDENTIFICATION NUMBER CFSI 82-18 and CFSI 83-7
8c. ADDRESS (City, State and ZIP Code) Air Force Systems Command Arnold Air Force Station, TN 37389-5000	10. SOURCE OF FUNDING NOS. PROGRAM ELEMENT NO.: D206VW PROJECT NO.: TASK NO.: WORK UNIT NO.:
11. TITLE (Include Security Classification) Please see reverse of this page.	
12. PERSONAL AUTHOR(S) Hindman, Richard G., The University of Texas at Arlington	
13a. TYPE OF REPORT Final	13b. TIME COVERED FROM 3/1/84 TO 2/28/85
14. DATE OF REPORT (Yr., Mo., Day) October 1985	15. PAGE COUNT 65
16. SUPPLEMENTARY NOTATION Available in Defense Technical Information Center (DTIC).	

17 COSATI CODES			18 SUBJECT TERMS (Continue on reverse if necessary and identify by block number)
FIELD	GROUP	SUB GR	
20	04		computational fluid dynamics axisymmetric flows two-dimensional flows
01	01		

19. ABSTRACT (Continue on reverse if necessary and identify by block number)

Theoretical background and several basic test cases are presented for a new, time-dependent Navier-Stokes solver for two-dimensional and axisymmetric flows. The goal of the effort is to invoke state-of-the-art computational fluid dynamics (CFD) technology to improve modeling of viscous phenomena and to increase the robustness of CFD analysis tools. The original motivation was inadequate representation of supersonic ramp-induced separation by existing CFD codes. The present work addresses that inadequacy by employing modern numerical methods which accurately model signal propagation in high-speed fluid flow.

The present technique solves the Navier-Stokes equations in general curvilinear coordinates in a four-sided domain bounded by a wall, an upper boundary opposite the wall, an inflow boundary, and an outflow boundary. The interior algorithm is a flux-difference splitting method similar to that of Yang, Lombard, and Bershader, but it is blended into a second order, implicit factored delta form. With implicitly treated boundary conditions,

20. DISTRIBUTION/AVAILABILITY OF ABSTRACT UNCLASSIFIED/UNLIMITED ☐ SAME AS RPT. ☒ OTIC USERS ☐	21. ABSTRACT SECURITY CLASSIFICATION Unclassified
22a. NAME OF RESPONSIBLE INDIVIDUAL W.O. Cole	22b TELEPHONE NUMBER (Include Area Code) (615) 454-7813 22c. OFFICE SYMBOL DOS

DD FORM 1473, 83 APR EDITION OF 1 JAN 73 IS OBSOLETE.

UNCLASSIFIED
SECURITY CLASSIFICATION OF THIS PAGE

11. TITLE. Concluded.

Development of a Two-Dimensional/Axisymmetric Implicit Navier-Stokes Solver Using Flux-Difference Splitting Concepts and Fully General Geometry

19. ABSTRACT. Concluded.

the solution is performed using a block tridiagonal method followed by an explicit updating of the boundaries. The resulting scheme satisfies the global conservation requirement to within the order of accuracy of the algorithm. The grid is generated using a relaxation Poisson solver. A systematic and rigorous development of the complete method is presented. Initial steps in code validation include successful reproduction of Couette and Blasius solutions.

PREFACE

The work reported herein was conducted by the author as principal investigator on subcontracts CFSI 82-18 and CFSI 83-7 between Iowa State University and Calspan Corporation/AEDC Division, operating contractor for the Aerospace Flight Dynamics testing effort at Arnold Engineering Development Center, Air Force Systems Command, Arnold Air Force Station, Tennessee. The work is a portion of the Supersonic and Hypersonic Computational Fluid Dynamics project, Project Number D206VW (V32A-B3). The Air Force Project Manager was Dr. Keith L. Kushman, AEDC/DOT. The manuscript was submitted for publication on April 30, 1985.

The author wishes to acknowledge the efforts of Mr. John O. Ievalts, a graduate student at Iowa State University, whose efforts on this work were invaluable.

CONTENTS

ILLUSTRATIONS

Figure Page

1.0 INTRODUCTION

Over the past decade, sufficient advances have been made in the field of computational fluid dynamics (CFD) to provide an extremely useful tool to engineering practitioners. This tool is the CFD technology which currently sees extensive use in a large variety of aerospace engineering design and analysis. The present report documents an application of this technology resulting in a new analysis tool (i.e., computer code) which is immediately applicable to the study of flow past specific components of modern aerospace vehicles. The present CFD development effort supports testing as well as analysis and evaluation of re-entry vehicles and high-speed aircraft. The specific technical problem addressed herein concerns viscous flow over a two-dimensional or axisymmetric body with possible streamwise separation.

1.1 MOTIVATION

Consider the wall/ramp arrangement shown in Fig. 1a. This two-dimensional configuration may represent a simple model of a vehicle control surface. A ramp-induced shock-boundary-layer interaction results when this model encounters a supersonic/hypersonic airstream. The flow separation resulting from this type of interaction can have devastating effects on the control surface performance. Therefore, it is of prime importance to be able to predict flows of this type accurately. Figure 1b illustrates a cylinder/flare configuration. Configurations of this type exist and also are subject to shock-induced separation problems. The present effort was motivated by an earlier, unpublished computational analysis at AEDC of ramp-induced separation on an actual re-entry vehicle control surface. The available Navier-Stokes solvers were found to underpredict the size of the separation zone by about a factor of two, even in laminar flow where the turbulence model is not involved. Since the separation zone is the primary phenomenon degrading RV flap performance at flight conditions, and since high Reynolds number phenomena are not adequately simulated in wind tunnels, it was deemed necessary to mount an assault on the problem with state-of-the-art CFD technology.

The result of the effort reported herein is a computer code designed to compute the viscous flow field on and about wall/ramp and cylinder/flare configurations. This code uses state-of-the-art CFD technology. To date the code has been tested against known solutions for Couette and Blasius flows and it has successfully reproduced the classical solutions. Preliminary solutions, not presented herein, have been obtained at AEDC for compressible, separated ramp flows.

1.2 BACKGROUND

Numerical computations to date have primarily been limited to the two-dimensional wall/ramp configurations. For example, Refs. 1 - 4 report numerical computations on problems of this type for both laminar and turbulent flows. Since this numerical work was reported, advances have been realized in the treatment of the inviscid terms of the descriptive equations. These advances provide for integration algorithms with substantially improved stability properties without the use of artificial viscosity. These more robust algorithms are capable of solving a tougher class of problems than previously possible. The remainder of this report documents the development of a pair of computer codes utilizing the new methods.

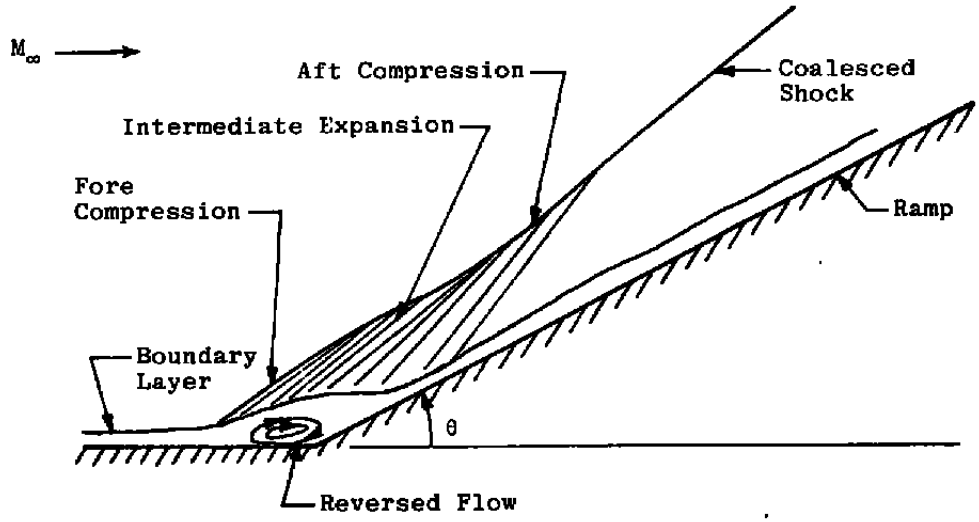

a. Ramp-induced shock-boundary layer interaction

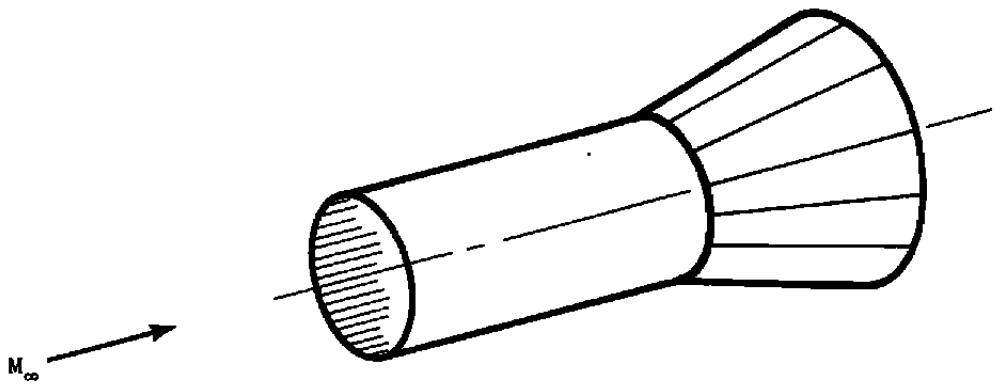

b. Hollow cylinder-flare configuration

Figure 1. Specific configurations of interest.

2.0 DESCRIPTIVE EQUATIONS

2.1 CARTESIAN COORDINATES

The two-dimensional Navier-Stokes equations expressed in Cartesian coordinates are given by

$$\frac{\partial \bar{\phi}}{\partial t} + \frac{\partial \bar{e}}{\partial x} + \frac{\partial \bar{f}}{\partial y} = 0 \tag{1}$$

where $\bar{e} = \bar{e}_i - \bar{e}_v$ and $\bar{f} = \bar{f}_i - \bar{f}_v$. $\bar{\phi}$ is the dependent variable vector and $\bar{e}$, $\bar{f}$ are the associated flux vectors. The bar indicates that these variables are defined with the use of the Cartesian velocity vector $\bar{q} = (\bar{u}, \bar{v})$. The inviscid and viscous contributions are indicated by a subscript i and v, respectively. Consult Ref. 5 for a precise definition of the vectors $\bar{\phi}$, $\bar{e}$, $\bar{f}$ in terms of the primitive flow variables. Equation (1) is valid only for 2-D flows. Axisymmetric flows are modeled by

$$\frac{\partial \phi}{\partial t} + \frac{\partial e}{\partial x} + \frac{\partial f}{\partial y} + h = 0 \tag{2}$$

where $e = e_i - e_v$, $f = f_i - f_v$, and $h = h_v$. Now ϕ is the dependent vvariable vector and f, g are the associated flux vectors. The source term, h, is inversely proportional to y, the radial coordinate. This term can easily be switched on for axisymmetric problems and off for 2-D problems. Note that the vectors ϕ, e, f, h are defined in terms of the cylindrical velocity vector q = (u, v). This results in the fact that ϕ, e, f appear identical to $\bar{\phi}$, $\bar{e}$, $\bar{f}$ when $\bar{u}$, $\bar{v}$ are replaced by u, v. It must also be recognized that $\nabla \cdot q$ appearing in the definitions for e, f (see Ref. 5) is given by

$$\nabla \cdot q = \frac{\partial u}{\partial x} + \frac{\partial v}{\partial y} + \frac{v}{y} \tag{3}$$

in contrast to $\nabla \cdot \bar{q}$ for $\bar{e}$, $\bar{f}$ given by

$$\nabla \cdot \bar{q} = \frac{\partial \bar{u}}{\partial x} + \frac{\partial \bar{v}}{\partial y}$$

2.2 GENERALIZED COORDINATES

An attempt has been made to construct as general a 2-D/axisymmetric Navier-Stokes solver as possible while maintaining a substantial degree of operational simplicity. The use

of generalized coordinates has contributed to this effort. Equation (2) is transformed from the (t,x,y) domain to the generalized (τ, ξ, η) computational domain to yield

$$\frac{\partial \phi}{\partial \tau} + \xi_t \frac{\partial \phi}{\partial \xi} + \xi_x \frac{\partial e}{\partial \xi} + \xi_y \frac{\partial f}{\partial \xi} + \eta_t \frac{\partial \phi}{\partial \eta} + \eta_x \frac{\partial e}{\partial \eta} + \eta_y \frac{\partial f}{\partial \eta} + h = 0 \tag{4}$$

where the following functional forms have been assumed:

$$\tau = t$$

$$\xi = \xi(t,x,y)$$

$$\eta = \eta(t,x,y)$$

This allows for the possibility of utilizing adaptive grids if so desired. The vectors ϕ, e_i, f_i, h_i, e_v, f_v, h_v are now given:

$$\phi = (\varrho, \varrho u, \varrho v, \varrho e)^T \tag{5a}$$

$$e_i = (\varrho u, p + \varrho u^2, \varrho uv, (p + \varrho e)u)^T \tag{5b}$$

$$f_i = (\varrho v, \varrho uv, p + \varrho v^2, (p + \varrho e)v)^T \tag{5c}$$

$$h_i = \frac{1}{y}(\varrho v, \varrho uv, \varrho v^2, (p + \varrho e)v)^T \tag{5d}$$

$$e_v = \begin{pmatrix} 0 \\ \lambda(\nabla \cdot q) + 2\mu(\xi_x u_\xi + \eta_x u_\eta) \\ \mu(\xi_x v_\xi + \eta_x v_\eta + \xi_y u_\xi + \eta_y u_\eta) \\ \lambda(\nabla \cdot q) u + 2\mu u (\xi_x u_\xi + \eta_x u_\eta) \\ + \mu v(\xi_x v_\xi + \eta_x v_\eta + \xi_y u_\xi + \eta_y u_\eta) + k(\xi_x T_\xi + \eta_x T_\eta) \end{pmatrix} \tag{5e}$$

$$f_v = \begin{pmatrix} 0 \\ \mu(\xi_y u_\xi + \eta_y u_\eta + \xi_x v_\xi + \eta_x v_\eta) \\ \lambda(\nabla \cdot q) + 2\mu(\xi_y v_\xi + \eta_y v_\eta) \\ \lambda(\nabla \cdot q)\, v + \mu u\,(\xi_y u_\xi + \eta_y u_\eta + \xi_x v_\xi + \eta_x v_\eta) \\ + 2\mu v(\xi_y v_\xi + \eta_y v_\eta) + k(\xi_y T_\xi + \eta_y T_\eta) \end{pmatrix} \tag{5f}$$

$$h_v = \frac{1}{y} \begin{pmatrix} 0 \\ \mu(\xi_y u_\xi + \eta_y u_\eta + \xi_x v_\xi + \eta_x v_\eta) \\ 2\mu(\xi_y v_\xi + \eta_y v_\eta) - 2\mu v/y \\ \lambda(\nabla \cdot q)\, v + \mu u\,(\xi_y u_\xi + \eta_y u_\eta + \xi_x v_\xi + \eta_x v_\eta) \\ + 2\mu v(\xi_y v_\xi + \eta_y v_\eta) + k(\xi_y T_\xi + \eta_y T_\eta) \end{pmatrix} \tag{5g}$$

2.3 CONFIGURATIONS OF SPECIFIC INTEREST

The flow problems of specific interest are those depicted in Fig. 1. Figure 1a illustrates a wall/ramp intersection encountering a high-speed viscous flow. The possible separation resulting from this complex interaction makes this problem of more than academic interest for aerospace vehicles in which control surfaces are used. Figure 1b illustrates a cylinder/flare configuration which exhibits similar separation characteristics but under different conditions due to the flow's radial relief. The current approach is to identify a computational region on these configurations and solve Eq. (4) on this domain subject to proper boundary conditions.

2.4 BOUNDARY CONDITIONS

In either the wall/ramp case or the cylinder/flare case the computational domain is illustrated in Fig. 2. The boundaries of this domain are labeled A,B,C,D corresponding to

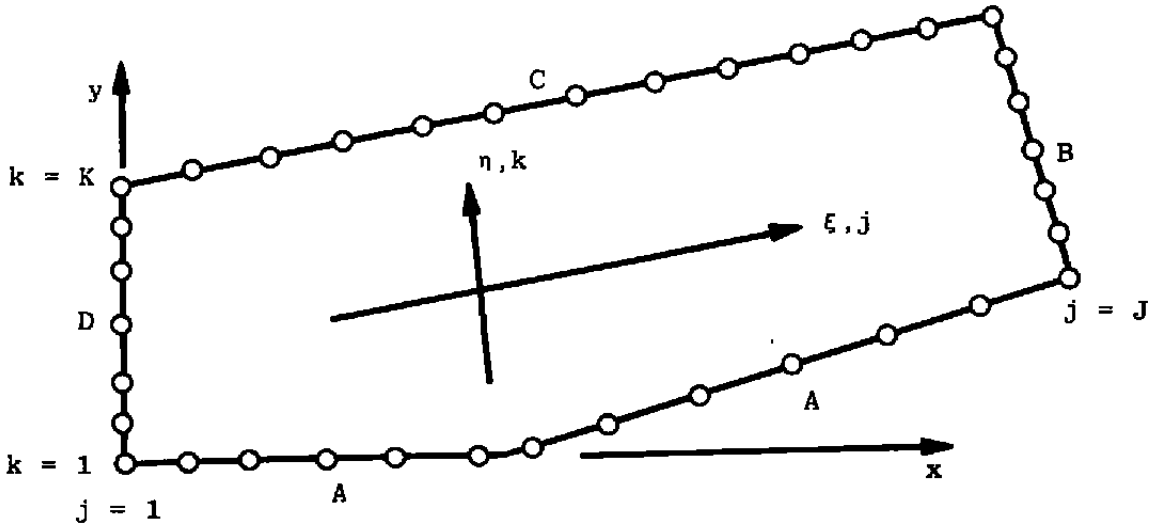

Figure 2. Computational domain layout.

body, outflow, upper, and inflow, respectively. Boundary conditions consistent with the viscous flow requirement are utilized on boundary A. That is, the no-slip condition requires $u = v = 0$ on this boundary. The surface temperature is either prescribed on this boundary or is determined from an adiabatic wall condition by the equation

$$\tilde{\alpha} \frac{\partial T}{\partial n} + (1 - \tilde{\alpha})(T - T_w) = 0$$

where T_w is the prescribed wall temperature value and T is the calculated wall temperature. $\tilde{\alpha}$ is 0 for the fixed wall case and 1 for the adiabatic case. Since n is the direction normal to the boundary A, it lies in the direction of $\nabla\eta$. The actual numerical implementation of this condition is reserved for Section 3.5. Finally, a condition on the normal pressure gradient is enforced to provide closure on the wall/ramp boundary. The simplest condition is $\partial p/\partial n = 0$ which is consistent with boundary-layer theory. Results illustrated in Ref. 5 show this to be adequate for the cases considered. However, Ref. 6 shows contrary results for a turbulent separated case near the reattachment region. For the present work in the interest of simplicity, the simple zero normal pressure gradient is enforced. For the more general case, the vector momentum equation is dotted with the normal direction $\nabla\eta$ to yield a rather complex expression for $\partial p/\partial n$ which must be solved for the wall pressure. This expression is given by

$$\frac{\partial p}{\partial n} = \frac{1}{\sqrt{\eta_x^2 + \eta_y^2}} \left\{ \left(\xi_x\eta_x + \xi_y\eta_y\right) \frac{\partial}{\partial \xi} \left[\lambda\left(\eta_x u_\eta + \eta_y v_\eta\right)\right] + 2\xi_x\eta_x \frac{\partial}{\partial \xi} \left(\mu\eta_x u_\eta\right) \right.$$

$$+ 2\xi_y\eta_y \frac{\partial}{\partial \xi}\left(\mu\eta_y v_\eta\right) + \left(\xi_x\eta_y + \xi_y\eta_x\right) \frac{\partial}{\partial \xi} \left[\mu\left(\eta_x v_\eta + \eta_y u_\eta\right)\right]$$

$$+ \left(\eta_x^2 + \eta_y^2\right) \frac{\partial}{\partial \eta} \left[\lambda\left(\nabla \cdot q\right)\right] + \eta_x^2 \frac{\partial}{\partial \eta} \left[2\mu\left(\xi_x u_\xi + \eta_x u_\eta\right)\right]$$

$$+ \eta_y^2 \frac{\partial}{\partial \eta} \left[2\mu\left(\xi_y v_\xi + \eta_y v_\eta\right)\right]$$

$$+ 2\eta_x\eta_y \frac{\partial}{\partial \eta} \left[\mu\left(\xi_x v_\xi + \xi_y u_\xi + \eta_x v_\eta + \eta_y u_\eta\right)\right]$$

$$\left. + \left(\eta_x^2 + \eta_y^2\right) \frac{\mu}{y} v_\eta + \frac{\eta_x\eta_y\mu}{y} u_\eta \right\} \tag{6}$$

This completes the ideology behind the viscous boundary conditions on boundary A. As mentioned, numerical implementation of these is discussed in Section 3.5.

Boundary B is an outflow boundary. The simplest treatment of boundaries of this type is to enforce either a zero streamwise first derivative or a zero streamwise second derivative of all dependent flow variables. This is stated as

$$\frac{\partial \phi}{\partial \xi} = 0$$

or

$$\frac{\partial^2 \phi}{\partial \xi^2} = 0 \tag{7}$$

This is equivalent to a zeroth order or first-order extrapolation of ϕ to boundary B from the interior of the domain along an η = constant curve. It should be noted that while this condition is simple and commonly used with success, it is not physically correct. This point is addressed further in Section 3.5.

Boundary C is generally thought of as having fixed dependent variables. However, an alternate option is considered in the present work. If flow exits the computational domain through boundary C, then it is technically correct to fix only one flow variable on this boundary. The rest must be computed from the descriptive equations. Pressure is chosen as the fixed variable for the present work.

Boundary D is an inflow boundary in which the dependent variables are fixed. This is technically correct from a signal propagation viewpoint only in the supersonic portion of this boundary. However, practice has demonstrated this to be an adequate boundary condition for flows of the type considered here.

The numerical aspects of all of these boundaries are best left for a discretized setting and are presented in Section 3.5.

3.0 DISCRETIZATION

3.1 GRID GENERATION AND METRICS

The numerical solution of Eq. (4) requires values for the metrics ξ_t, η_t, ξ_x, η_x, ξ_y, η_y. The time metrics are zero for the present work since a moving grid is not presently considered. The remaining metrics are obtained from the grid point locations and the metric identities.

$$\xi_x = \frac{\bar{r}_\eta \times \bar{r}_\zeta \cdot \hat{i}}{J} = \frac{y_\eta}{J}$$

$$\xi_y = \frac{\bar{r}_\eta \times \bar{r}_\zeta \cdot \hat{j}}{J} = -\frac{x_\eta}{J}$$

$$\eta_x = \frac{\bar{r}_\zeta \times \bar{r}_\xi \cdot \hat{i}}{J} = -\frac{y_\xi}{J}$$

$$\eta_y = \frac{\bar{r}_\zeta \times \bar{r}_\xi \cdot \hat{j}}{J} = \frac{x_\xi}{J} \tag{8a}$$

where

$$J = \bar{r}_\xi \times \bar{r}_\eta \cdot \bar{r}_\zeta = x_\xi y_\eta - x_\eta y_\xi \tag{8b}$$

since for this 2-D domain $\zeta = z$ and $\bar{r}_\zeta = (0, 0, 1)$. Now since all calculations are performed in the computational domain, these metrics are easily computed once the values of x_ξ, y_ξ, x_η,

y_η are known. These values are determined with finite difference formulae. The particular formulae chosen depend upon how the flux derivatives are treated. A discussion of this is reserved for Section 3.4 but regardless of the specific formulae chosen, the grid point locations must first be known.

The approach used in the present work is to break the grid generation problem up into four distinct parts:

1. Boundary point distribution
2. Forcing function calculation
3. Relaxation
4. Redistribution

Each of these is now discussed. Boundary point distribution simply means that the analyst decides where to place the grid points on all four computational boundaries beginning at boundary A and moving counterclockwise to boundary D (refer to Fig. 2). The analyst must create the (x,y) coordinate values for each grid point in this counterclockwise cycle. This is typically accomplished by a separate computer program which distributes points on the boundaries according to some measure of expected flow field activity. The points need only to be equally spaced on boundaries B and D at this time since the redistribution phase redistributes points along all ξ = constant curves according to an input from the analyst regarding boundary-layer resolution. If J,K are used to represent the number of points in the ξ, η directions, respectively, and j,k are the indices of these points, then part 1 of the grid generation process produces

$$x_{j,1},\ y_{j,1} \text{ for } j = 1, 2, \ldots, J$$

$$x_{J,k},\ y_{J,k} \text{ for } k = 1, 2, \ldots, K$$

$$x_{j,K},\ y_{j,K} \text{ for } j = 1, 2, \ldots, J$$

$$x_{1,k},\ y_{1,k} \text{ for } k = 1, 2, \ldots, K$$

See Fig. 2 for reference. Part 2 of the grid generation process uses the work of Ref. 7 to force the interior points in the grid to respond to the boundary point distribution created in part 1. The general grid generation approach used is due to Refs. 8–9 in which two coupled Poisson-type partial differential equations are solved for the x,y values at all interior points given the

x,y values on the boundaries. The grid equations

$$\nabla^2 \xi = P(\xi, \eta)$$

$$\nabla^2 \eta = Q(\xi, \eta)$$

are expressed in computational space as

$$\alpha \bar{r}_{\xi\xi} - 2\beta \bar{r}_{\xi\eta} + \gamma \bar{r}_{\eta\eta} + J^2 P \bar{r}_{\xi} + J^2 Q \bar{r}_{\eta} = 0 \tag{9}$$

where $\bar{r} = (x,y)$, $\alpha = x_\eta^2 + y_\eta^2$, $\beta = x_\xi x_\eta + y_\xi y_\eta$, and $\gamma = x_\xi^2 + y_\xi^2$. Equation (9) represents two coupled equations which are solved by relaxation once the functions P, Q are determined. These functions, in general, provide for arbitrary point clustering but in the present work are used to force interior points to respond to boundary point placement as suggested in Ref. 7. Again, using the index notation, the P, Q functions are defined as

$$P = \Phi(\xi,\eta) \, |\nabla \xi|^2$$

$$Q = \psi(\xi, \eta) \, |\nabla \eta|^2$$

where $\Phi(\xi, \eta)$, $\psi(\xi, \eta)$ are determined strictly from boundary point information as follows. Along boundary A, Φ is defined as

$$\Phi(\xi, \eta = 1) = - \frac{s_{\xi\xi}}{s_\xi}$$

or

$$\Phi_{j,1} = - 2(s_{j+1} + s_{j-1} - 2s_j)/(s_{j+1} - s_{j-1}) \tag{10a}$$

in finite-difference form. Note that $\xi = j$, $\eta = k$ are assumed so that $\Delta\xi = \Delta\eta = 1$. The s in these equations is simply the arc length along the boundary. This is determined by evaluating the quadrature

$$s_j = \int_1^{\xi_j} \sqrt{(x_\xi^2 + y_\xi^2)_{j,1}} \, d\xi$$

Likewise on boundary C,

$$\Phi_{j,K} = - 2(s_{j+1} + s_{j-1} - 2s_j)/(s_{j+1} - s_{j-1}) \tag{10b}$$

where

$$s_j = \int_1^{\xi_j} \sqrt{(x_\xi^2 + y_\xi^2)_{j,K}}\, d\xi$$

Equations (10a) and (10b) are applied only to interior boundary points (i.e., j = 2, 3, ..., J − 1). The interior field values of Φ at j for k = 2, ..., K − 1 are simply found from the interpolation formula

$$\Phi_{j,k} = \Phi_{j,1} + \left(\frac{k-1}{K-1}\right)\left(\Phi_{j,K} - \Phi_{j,1}\right)$$

for j = 2, 3, ..., J − 1 and k = 2, 3, ..., K − 1. On boundary B,

$$\psi_{J,k} = -2(s_{k+1} + s_{k-1} - 2s_k)/(s_{k+1} - s_{k-1})$$

where

$$s_k = \int_1^{\eta_k} \sqrt{(x_\eta^2 + y_\eta^2)_{J,k}}\, d\eta$$

and on boundary D,

$$\psi_{1,k} = -2(s_{k+1} + s_{k-1} - 2s_k)/(s_{k+1} - s_{k-1})$$

where

$$s_k = \int_1^{\eta_k} \sqrt{(x_\eta^2 + y_\eta^2)_{1,k}}\, d\eta$$

Then for the interior grid points

$$\psi_{j,k} = \psi_{1,k} + \left(\frac{j-1}{J-1}\right)\left(\psi_{J,k} - \psi_{1,k}\right)$$

for j = 2, 3, ..., J − 1 and k = 2, 3, ..., K − 1. Now, Φ, ψ are known at all interior grid points. An initial grid is then prescribed to begin the relaxation process. The P,Q functions are computed as indicated from Φ, ψ and $\nabla\xi$, $\nabla\eta$. Part 3 of the grid generation process is then carried out to produce a converged grid. The grid resulting from this process will not be sufficiently refined near the η = 1 boundary to resolve the viscous features of the flow field.

The redistribution process in part 4 is designed to resolve this deficiency. Following part 3, a grid such as that shown in Fig. 3 is produced. The points are now redistributed along each ξ = constant curve to satisfy some user prescribed near wall point spacing. Consider the ξ = constant curve given by $\xi = 4$ in Fig. 3. The first requirement of the redistribution process is that the same total arc length be reproduced. This arc length is computed by

$$S_j = \int_{\eta=1}^{\eta=K} \sqrt{(x_\eta^2 + y_\eta^2)_{j,k}}\, d\eta$$

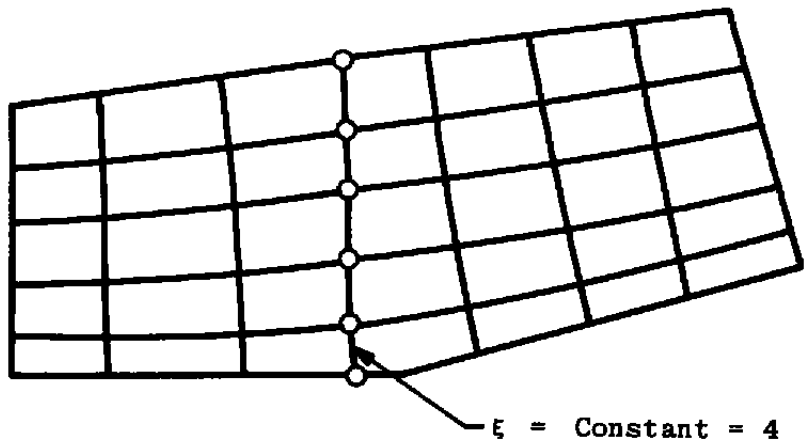

Figure 3. Redistribution along ξ = constant lines.

In general, the desire of the present work is to redistribute points to satisfy the relation (see Ref. 10)

$$s_j(\eta) = G_j(\eta) S_j \tag{11a}$$

where

$$G_j(\eta) = 1 - \beta_j \left[\frac{\left(\frac{\beta_j + 1}{\beta_j - 1}\right)^{1-\bar{\eta}} - 1}{\left(\frac{\beta_j + 1}{\beta_j - 1}\right)^{1-\bar{\eta}} + 1} \right] \tag{11b}$$

with $\bar{\eta} = (\eta - 1)/K - 1)$. This is to be subject to the constraint that $s_j(2) = \Delta s_j$ which is prescribed by the analyst as direct control of the point spacing near the wall. Then application of this constraint to Eq. (11) yields

$$1 - \frac{\Delta s_j}{S_j} = \beta_j \left[\frac{\left(\frac{\beta_j + 1}{\beta_j - 1} \right)^{1-\bar{\eta}_2} - 1}{\left(\frac{\beta_j + 1}{\beta_j - 1} \right)^{1-\bar{\eta}_2} + 1} \right] \tag{12}$$

where

$$\bar{\eta}_2 = \left(\frac{1}{K - 1} \right)$$

The value of β_j is then determined from this equation using a Newton-Raphson iteration. The points along each ξ = constant curve are then redistributed using these β_j values in Eq. (11) and the grid generation process is complete. An example of a grid generated by this method is illustrated in Fig. 4.

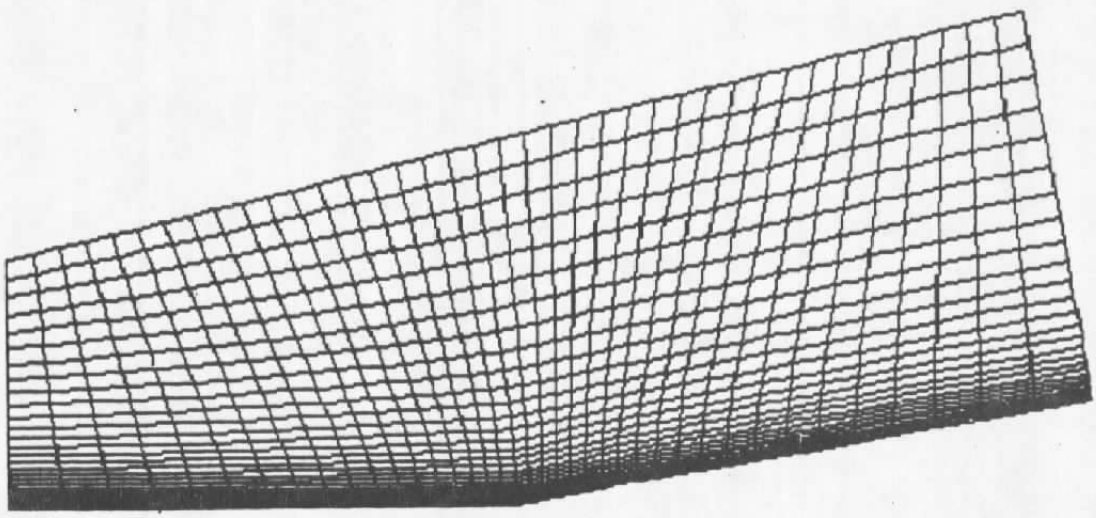

Figure 4. Completed grid.

3.2 FLUX DIFFERENCE SPLITTING

The concept of splitting the convection terms was introduced at least as early as 1952 in Ref. 11. Since then the idea has been expanded in a number of ways by various investigators (see Refs. 12–19). The flux difference splitting concept used in the present work closely resembles that of Ref. 19 but the present work blends this concept into the framework of the implicit solution of the Navier-Stokes equations in factored delta form and the splitting concepts are developed in a more systematic and rigorous fashion than in Ref. 19.

Consider Eq. (4) expressed in the form

$$\frac{\partial \phi}{\partial \tau} + \left(\xi_t \frac{\partial \phi}{\partial \xi} + \xi_x \frac{\partial e_i}{\partial \xi} + \xi_y \frac{\partial f_i}{\partial \xi} \right) + \left(\eta_t \frac{\partial \phi}{\partial \eta} + \eta_x \frac{\partial e_i}{\partial \eta} + \eta_y \frac{\partial f_i}{\partial \eta} \right) + h_i$$

$$= \xi_x \frac{\partial e_v}{\partial \xi} + \xi_y \frac{\partial f_v}{\partial \xi} + \eta_x \frac{\partial e_v}{\partial \eta} + \eta_y \frac{\partial f_v}{\partial \eta} + h_v \tag{13}$$

Let A, B represent the Jacobian matrices

$$\frac{\partial e_i}{\partial \phi}, \frac{\partial f_i}{\partial \phi}$$

respectively and let $A^* = \xi_t I + \xi_x A + \xi_y B$ and $B^* = \eta_t I + \eta_x A + \eta_y B$ where I is the identity matrix. Then Eq. (13) becomes

$$\frac{\partial \phi}{\partial \tau} + A^* \frac{\partial \phi}{\partial \xi} + B^* \frac{\partial \phi}{\partial \eta} + h_i = \xi_x \frac{\partial e_v}{\partial \xi} + \xi_y \frac{\partial f_v}{\partial \xi} + \eta_x \frac{\partial e_v}{\partial \eta} + \frac{\partial f_v}{\partial \eta} + h_v \tag{14}$$

For an inviscid problem, the right-hand side of Eq. (14) is zero and the matrices A^*,B^* determine the characteristic structure of the resulting hyperbolic system. It is for this reason that the splitting concept in the present work is applied only to the inviscid terms. The diffusive terms on the right side of Eq. (14) are not considered to contribute to the signal propagation direction information in the fluid. Note, however, that the viscous contribution does, in fact, include terms which can be expressed as first derivatives of ϕ multiplied by various functions implicitly dependent upon ϕ for the case of an axisymmetric problem. For example, derivatives of e_v and f_v which involve $\nabla \cdot q$ contribute due to the v/y term existing in $\nabla \cdot q$. A portion of the h_v term also contributes. It is therefore possible to include these contributions in the matrices A^* and B^*, thereby altering the characteristic structure of the governing equations. However, as mentioned, this idea was avoided in the present work.

The development of the split equation requires first that the system's characteristic structure be exploited in detail. This is accomplished by diagonalizing A^* and B^* as follows. Let T_ξ^{-1} represent the matrix whose rows are the left eigenvectors of A^*. Let T_ξ represent the matrix whose columns are the right eigenvectors of A^*, and let Λ_ξ represent the diagonal matrix whose nonzero elements are the eigenvalues of A^*. Likewise let T_η^{-1}, T_η, Λ_η represent left eigenvector, right eigenvector, and diagonal eigenvalue matrices of the matrix B^*. The A^*, B^* can be expressed as

$$A^* = T_\xi \Lambda_\xi T_\xi^{-1},\ B^* = T_\eta \Lambda_\eta T_\eta^{-1} \tag{15}$$

Since

$$A^* \frac{\partial \phi}{\partial \xi} = \xi_t \frac{\partial \phi}{\partial \xi} + \xi_x \frac{\partial e_i}{\partial \xi} + \xi_y \frac{\partial f_i}{\partial \xi}$$

and

$$B^* \frac{\partial \phi}{\partial \eta} = \eta_t \frac{\partial \phi}{\partial \eta} + \eta_x \frac{\partial e_i}{\partial \eta} + \eta_y \frac{\partial f_i}{\partial \eta}$$

the quantities $\partial\phi/\partial\xi$, $\partial\phi/\partial\eta$ may be expressed as

$$\frac{\partial \phi}{\partial \xi} = A^{*-1}\left(\xi_t \frac{\partial \phi}{\partial \xi} + \xi_x \frac{\partial e_i}{\partial \xi} + \xi_y \frac{\partial f_i}{\partial \xi} \right) \tag{16a}$$

$$\frac{\partial \phi}{\partial \eta} = B^{*-1}\left(\eta_t \frac{\partial \phi}{\partial \eta} + \eta_x \frac{\partial e_i}{\partial \eta} + \eta_y \frac{\partial f_i}{\partial \eta} \right) \tag{16b}$$

But from Eq. (15),

$$A^{*-1} = T_\xi \Lambda_\xi^{-1} T_\xi^{-1} \tag{17a}$$

$$B^{*-1} = T_\eta \Lambda_\eta^{-1} T_\eta^{-1} \tag{17b}$$

Equation (14) requires the product $A^* \partial\phi/\partial\xi$, which becomes

$$T_\xi \Lambda_\xi T_\xi^{-1} \frac{\partial \phi}{\partial \xi} \tag{18}$$

by substitution of Eq. (15). This term may now be split into a part involving positive eigenvalues plus a part involving negative eigenvalues. This is desired for the purpose of determining which grid points to use in finite-differencing the ξ derivatives in order to maintain consistency with the preferred propagation directions in the hyperbolic part of the governing equations. Since Λ_ξ is the diagonal matrix of eigenvalues, let Λ_ξ^+, Λ_ξ^- represent the parts involving positive and negative eigenvalues, respectively. Then

$$\Lambda_\xi = \Lambda_\xi^+ + \Lambda_\xi^-$$

and Eq. (18) becomes

$$T_\xi \Lambda_\xi^+ T_\xi^{-1} \frac{\partial \phi}{\partial \xi} + T_\xi \Lambda_\xi^- T_\xi^{-1} \frac{\partial \phi}{\partial \xi}$$

which by substitution from Eqs. (16a) and (17a) becomes

$$T_\xi \Lambda_\xi^+ \Lambda_\xi^{-1} T_\xi^{-1} \left(\xi_t \frac{\partial \phi}{\partial \xi} + \xi_x \frac{\partial e_i}{\partial \xi} + \xi_y \frac{\partial f_i}{\partial \xi} \right)$$

$$+ T_\xi \Lambda_\xi^- \Lambda_\xi^{-1} T_\xi^{-1} \left(\xi_t \frac{\partial \phi}{\partial \xi} + \xi_x \frac{\partial e_i}{\partial \xi} + \xi_y \frac{\partial f_i}{\partial \xi} \right)$$

or

$$Q^+ \left(\xi_t \frac{\partial \phi}{\partial \xi} + \xi_x \frac{\partial e_i}{\partial \xi} + \xi_y \frac{\partial f_i}{\partial \xi} \right) + Q^- \left(\xi_t \frac{\partial \phi}{\partial \xi} + \xi_x \frac{\partial e_i}{\partial \xi} + \xi_y \frac{\partial f_i}{\partial \xi} \right)$$

with the help of the definitions

$$Q^+ = T_\xi \Lambda_\xi^+ \Lambda_\xi^{-1} T_\xi^{-1} \qquad Q^- = T_\xi \Lambda_\xi^- \Lambda_\xi^{-1} T_\xi^{-1}$$

Now an identical treatment of the B* term in Eq. (14) with the definitions

$$R^+ = T_\eta \Lambda_\eta^+ \Lambda_\eta^{-1} T_\eta^{-1} \qquad R^- = T_\eta \Lambda_\eta^- \Lambda_\eta^{-1} T_\eta^{-1}$$

yields the continuous but split version of Eq. (14).

$$\frac{\partial \phi}{\partial \tau} + Q^+ \left(\xi_t \frac{\partial \phi}{\partial \xi} + \xi_x \frac{\partial e_i}{\partial \xi} + \xi_y \frac{\partial f_i}{\partial \xi} \right) + Q^- \left(\xi_t \frac{\partial \phi}{\partial \xi} + \xi_x \frac{\partial e_i}{\partial \xi} + \xi_y \frac{\partial f_i}{\partial \xi} \right)$$

$$+ R^+ \left(\eta_t \frac{\partial \phi}{\partial \eta} + \eta_x \frac{\partial e_i}{\partial \eta} + \eta_y \frac{\partial f_i}{\partial \eta} \right) + R^- \left(\eta_t \frac{\partial \phi}{\partial \eta} + \eta_x \frac{\partial e_i}{\partial \eta} \right.$$

$$\left. + \eta_y \frac{\partial f_i}{\partial \eta} \right) + h_i = \xi_x \frac{\partial e_v}{\partial \xi} + \xi_y \frac{\partial f_v}{\partial \xi} + \eta_x \frac{\partial e_v}{\partial \eta} + \eta_y \frac{\partial f_v}{\partial \eta} + h_v \qquad (19)$$

The inviscid counterpart of Eq. (19) is presented in Ref. 19. The present development of this equation is, however, entirely different from that of Ref. 19. Clearly for Eq. (19) to be consistent, the following requirements hold

$$Q^+ + Q^- = I$$

$$R^+ + R^- = I$$

Note that the construction of Q^+, Q^-, R^+, R^- requires an inverse of diagonal eigenvalue matrices. Consider Q^+ for example,

$$Q^+ = T_\xi \Lambda_\xi^+ \Lambda_\xi^{-1} T_\xi^{-1}$$

and

$$\Lambda_\xi = \text{diag}\left(\xi_t + \xi_x u + \xi_y v,\ \xi_t + \xi_x u + \xi_y v,\ \xi_t + \xi_x u + \xi_y v\right.$$

$$\left. + c\sqrt{\xi_x^2 + \xi_y^2},\ \xi_t + \xi_x u + \xi_y v - c\sqrt{\xi_x^2 + \xi_y^2}\right)$$

where c is the sonic velocity of the fluid. The inverse of Λ_ξ does not exist if $\xi_t + \xi_x u + \xi_y v = 0$ or $| \xi_t + \xi_x u + \xi_y v | = c\sqrt{\xi_x^2 + \xi_y^2}$. To prevent these circumstances from causing difficulties, the products $\Lambda_\xi^+ \Lambda_\xi^{-1}$ and $\Lambda_\xi^- \Lambda_\xi^{-1}$ are treated in the following way. Let $\Lambda_\xi = \text{diag}\,(\lambda_1, \lambda_2, \lambda_3, \lambda_4)$ and let $\hat{\Lambda}_\xi^+ = \Lambda_\xi^+ \Lambda_\xi^{-1} = \text{diag}\,(\lambda_1^+/\lambda_1, \lambda_2^+/\lambda_2, \lambda_3^+/\lambda_3, \lambda_4^+/\lambda_4)$. Then

$$\lambda_i^+/\lambda_i = \hat{\lambda}_i^+ = \begin{cases} 0 & \lambda_i < 0 \\ 1/2 & \lambda_i = 0 \\ 1 & \lambda_i > 0 \end{cases} \quad \text{for } i = 1,2,3,4 \tag{20a}$$

Likewise,

$$\lambda_i^-/\lambda_i = \hat{\lambda}_i^- = \begin{cases} 0 & \lambda_i > 0 \\ 1/2 & \lambda_i = 0 \\ 1 & \lambda_i < 0 \end{cases} \quad \text{for } i = 1,2,3,4$$

This way, the singular character of the eigenvalue matrices at selected points is avoided. The same procedure is used to determine R^+ and R^- corresponding to the η direction.

Equation (19) has some very special features. First, the matrices Q^+, Q^-, R^+, R^- act as complex weight factors weighting the various fluid signals (waves) according to the appropriate propagation directions. This is accomplished in a discretized setting by using backward finite-difference approximations for derivatives weighted by positive eigenvalues and forward finite-differences for derivatives weighted by negative eigenvalues. This is consistent with the wave propagation physics since positive eigenvalues mean characteristic signal paths toward the positive coordinate direction with the opposite true for negative eigenvalues. In addition to this characteristic-like structure, the equation retains its conservation law form, thus providing a needed shock-capturing capability to the resulting algorithm. See Ref. 20 for a discussion of the connection between conservation law form and the computation of weak solutions.

3.3 INTEGRATION SCHEME

The implicit integration algorithm used in the present work is developed in this section. Before beginning the development, some comments regarding notation are in order. Variables are generally functions of (τ, ξ, η). Thus, when writing a variable it is important to identify which value of τ and at which point in space (ξ, η) the variable is applicable. Generally this is accomplished in discrete work with an index notation. In this work, an n superscript is used for the τ index and j, k subscripts are used for the ξ, η indices, respectively. Therefore, the variable ϕ at the point $\xi = j\Delta\xi$, $\eta = k\Delta\eta$ and $\tau = n\Delta\tau$ would be identified by $\phi^n_{j,k}$ where $\Delta\xi$, $\Delta\eta$, and $\Delta\tau$ are the computational grid point spacings and the time increment, respectively. Because of the notational complexity of this and other sections, a shorthand notation is followed. If the term ϕ is encountered with no indices, it is assumed to be $\phi^n_{j,k}$. If ϕ_{j+1} is encountered, the τ index is assumed to be n and the η index is assumed to be k. Simply put, only indices not equal to n, j, k are explicitly written. This approach greatly enhances the readability of this and other sections. In addition, the symbols Δ, ∇ imply first-order forward and backward differences, respectively. No subscript implies differencing in the τ coordinate and ξ, η subscripts imply general differencing in the ξ, η coordinates.

With this notation, consider the equation

$$\phi^{n+1} = \phi + (1 - \beta)\Delta\tau\,\phi_\tau + \beta\Delta\tau\,\phi_\tau^{n+1} \tag{21}$$

If $\beta = 0$ an Euler explicit scheme results, $\beta = 1/2$ corresponds to trapezoidal time differencing, and $\beta = 1$ gives Euler implicit differencing. Consider ϕ_τ^{n+1} from Eq. (19).

$$
\begin{aligned}
-\phi_\tau^{n+1} = {} & \left[Q^+ + Q^-\right]\left[\xi_t^{n+1}\frac{\partial}{\partial\xi}\left(\phi + \Delta\phi + 0(\Delta^2)\right)\right. \\
& + \xi_x^{n+1}\frac{\partial}{\partial\xi}\left(e_i + A\Delta\phi + 0(\Delta^2)\right) \\
& \left. + \xi_y^{n+1}\frac{\partial}{\partial\xi}\left(f_i + B\Delta\phi + 0(\Delta^2)\right)\right] \\
& + \left[R^+ + R^-\right]\left[\eta_t^{n+1}\frac{\partial}{\partial\eta}\left(\phi + \Delta\phi + 0(\Delta^2)\right)\right. \\
& + \eta_x^{n+1}\frac{\partial}{\partial\eta}\left(e_i + A\Delta\phi + 0(\Delta^2)\right) \\
& \left. + \eta_y^{n+1}\frac{\partial}{\partial\eta}\left(f_i + B\Delta\phi + 0(\Delta^2)\right)\right] + h_i^{n+1} \\
& - \left[\xi_x^{n+1}\frac{\partial e_v^{n+1}}{\partial\xi} + \xi_y^{n+1}\frac{\partial f_v^{n+1}}{\partial\xi} + \eta_x^{n+1}\frac{\partial e_v^{n+1}}{\partial\eta} + \eta_y^{n+1}\frac{\partial f_v^{n+1}}{\partial\eta} + h_v^{n+1}\right]
\end{aligned}
\tag{22}
$$

Note that $Q^+ + Q^-$ may be evaluated at n or n + 1 since in either case the result is the identity matrix. Now with the additional linearizations

$$h_i^{n+1} = h_i + H_i\Delta\phi + 0(\Delta^2)$$

$$e_v^{n+1} = e_v + C\Delta\phi + 0(\Delta^2)$$

$$f_v^{n+1} = f_v + D\Delta\phi + 0(\Delta^2)$$

$$h_v^{n+1} = h_v + H_v\Delta\phi + 0(\Delta^2)$$

where

$$H_i = \frac{\partial h_i}{\partial\phi}$$

$$C = \frac{\partial e_v}{\partial \phi}$$

$$D = \frac{\partial f_v}{\partial \phi}$$

and

$$H_v = \frac{\partial h_v}{\partial \phi}$$

and also

$$\xi_t^{n+1} = \xi_t + \Delta\xi_t \qquad \eta_x^{n+1} = \eta_x + \Delta\eta_x$$

$$\eta_t^{n+1} = \eta_t + \Delta\eta_t \qquad \xi_y^{n+1} = \xi_y + \Delta\xi_y$$

$$\xi_x^{n+1} = \xi_x + \Delta\xi_x \qquad \eta_y^{n+1} = \eta_y + \Delta\eta_y$$

substitution into Eq. (22) yields

$$-\phi_\tau^{n+1} = \left\{\left[\left(Q^+ + Q^-\right)\left(\xi_t \frac{\partial}{\partial\xi} I + \xi_x \frac{\partial}{\partial\xi} A + \xi_y \frac{\partial}{\partial\xi} B\right) + \left(R^+ + R^-\right)\right.\right.$$

$$\left.\left(\eta_t \frac{\partial}{\partial\eta} I + \eta_x \frac{\partial}{\partial\eta} A + \eta_y \frac{\partial}{\partial\eta} B\right) + H_i\right]$$

$$\left. - \left[\xi_x \frac{\partial}{\partial\xi} C + \xi_y \frac{\partial}{\partial\xi} D + \eta_x \frac{\partial}{\partial\eta} C + \eta_y \frac{\partial}{\partial\eta} D + H_v\right]\right\}\Delta\phi - \phi_\tau$$

$$+ \left(Q^+ + Q^-\right)\left(\Delta\xi_t\phi_\xi + \Delta\xi_x e_{i_\xi} + \Delta\xi_y f_{i_\xi}\right) + \left(R^+ + R^-\right)$$

$$\left(\Delta\eta_t\phi_\eta + \Delta\eta_x e_{i_\eta} + \Delta\eta_y f_{i_\eta}\right)$$

$$- \left[\Delta\xi_x e_{v_\xi} + \Delta\xi_y f_{v_\xi} + \Delta\eta_x e_{v_\eta} + \Delta\eta_y f_{v_\eta}\right] + 0(\Delta^2)$$

where all terms of $0(\Delta^2)$ were ignored. Substitution of this result into Eq. (21) gives

$$\left\{I + \beta\Delta\tau\left[\left(Q^+ + Q^-\right)\left(\xi_t \frac{\partial}{\partial\xi} I + \xi_x \frac{\partial}{\partial\xi} A + \xi_y \frac{\partial}{\partial\xi} B\right) + \left(R^+ + R^-\right)\right.\right.$$

$$\left(\eta_t \frac{\partial}{\partial\eta} I + \eta_x \frac{\partial}{\partial\eta} A + \eta_y \frac{\partial}{\partial\eta} B\right) + H_i - \left(\xi_x \frac{\partial}{\partial\xi} C + \xi_y \frac{\partial}{\partial\xi} D + \eta_x \frac{\partial}{\partial\eta} C\right.$$

$$\left.\left. + \eta_y \frac{\partial}{\partial\eta} D + H_v\right)\right]\right\}\Delta\phi = \Delta\tau\phi_\tau - \bar{\beta}\Delta\tau\left[\left(Q^+ + Q^-\right)\left(\Delta\xi_t\phi_\xi + \Delta\xi_x e_{i_\xi}\right.\right. \quad (23)$$

$$\left.\left. + \Delta\xi_y f_{i_\xi}\right) + \left(R^+ + R^-\right)\left(\Delta\eta_t\phi_\eta + \Delta\eta_x e_{i_\eta} + \Delta\eta_y f_{i_\eta}\right)\right]$$

$$+ \bar{\beta}\Delta\tau\left(\Delta\xi_x e_{v_\xi} + \Delta\xi_y f_{v_\xi} + \Delta\eta_x e_{v_\eta} + \Delta\eta_y f_{v_\eta}\right) + 0(\Delta^2)$$

Equation (23) represents the general time differencing formula for interior points of the computational domain. This scheme is second-order accurate in τ if $\bar{\beta}$, $\beta = 1/2$. The spatial accuracy of the steady-state solution is dependent only upon the ξ, η differences used on the right-hand side of Eq. (23). It should be noted that only first-order spatial difference approximations are required on the left side of Eq. (23) to maintain an accuracy consistent with the second-order time differencing. If the transient accuracy of the solution is not of primary importance, it is worthwhile to drop the source terms and viscous terms on the left side of Eq. (23). The result is first-order accurate in τ, and good stability properties remain so long as the convective terms are treated according to the splitting philosophy. The result of dropping these terms and factoring the remaining operator yields

$$\left[I + \beta\Delta\tau\, Q^+\left(\xi_t\nabla_\xi I + \xi_x\nabla_\xi A + \xi_y\nabla_\xi B\right) + \beta\Delta\tau\, Q^-\left(\xi_t\Delta_\xi I + \xi_x\Delta_\xi A + \xi_y\Delta_\xi B\right)\right]$$

$$\times\left[I + \beta\Delta\tau\, R^+\left(\eta_t\nabla_\eta I + \eta_x\nabla_\eta A + \eta_y\nabla_\eta B\right)\right.$$

$$\left. + \beta\Delta\tau\, R^-\left(\eta_t\Delta_\eta I + \eta_x\Delta_\eta A + \eta_y\Delta_\eta B\right)\right]\Delta\phi$$

$$= \Delta\tau\phi_\tau + \bar{\beta}\Delta\tau\Big(\Delta\xi_x\delta_\xi e_v + \Delta\xi_y\delta_\xi f_v + \Delta\eta_x\delta_\eta e_v + \Delta\eta_y\delta_\eta f_v\Big)$$

$$- \bar{\beta}\Delta\tau\Big[Q^+\Big(\Delta\xi_t\nabla_\xi\phi + \Delta\xi_x\nabla_\xi e_i + \Delta\xi_y\nabla_\xi f_i\Big) + Q^-\Big(\Delta\xi_t\Delta_\xi\phi + \Delta\xi_x\Delta_\xi e_i + \Delta\xi_y\Delta_\xi f_i\Big)$$

$$+ R^+\Big(\Delta\eta_t\nabla_\eta\phi + \Delta\eta_x\nabla_\eta e_i + \Delta\eta_y\nabla_\eta f_i\Big) + R^-\Big(\Delta\eta_t\Delta_\eta\phi + \Delta\eta_x\Delta_\eta e_i + \Delta\eta_y\Delta_\eta f_i\Big)\Big] \tag{24a}$$

where ϕ_τ is given by solving Eq. (19) to yield

$$\phi_\tau = \Big(\xi_x\delta_\xi e_v + \xi_y\delta_\xi f_v + \eta_x\delta_\eta e_v + \eta_y\delta_\eta f_v + h_v\Big)$$

$$- \Big[Q^+\Big(\xi_t\Gamma_\xi^+\phi + \xi_x\Gamma_\xi^+ e_i + \xi_y\Gamma_\xi^+ f_i\Big)$$

$$+ Q^-\Big(\xi_t\Gamma_\xi^-\phi + \xi_x\Gamma_\xi^- e_i + \xi_y\Gamma_\xi^- f_i\Big)$$

$$+ R^+\Big(\eta_t\Gamma_\eta^+\phi + \eta_x\Gamma_\eta^+ e_i + \eta_y\Gamma_\eta^+ f_i\Big)$$

$$+ R^-\Big(\eta_t\Gamma_\eta^-\phi + \eta_x\Gamma_\eta^- e_i + \eta_y\Gamma_\eta^- f_i\Big) + h_i\Big]$$

The factoring introduces an error of the same order as the error in the second-order differencing scheme which is appropriately ignored. The operators δ_ξ, δ_η are difference operators used with the diffusive terms and are now precisely defined. Consider the typical term $\delta_\xi e_v$. A quick look at Eq. (5e) reveals that $\delta_\xi e_v$ will always take one of three forms. Any of

$$\delta_\xi\Big(cg\frac{\partial}{\partial\xi}s\Big), \quad \delta_\xi\Big(cg\frac{\partial}{\partial\eta}s\Big), \quad \text{or } \delta_\xi\Big(sg\Big) \tag{25}$$

where c and s represent quantities dependent only upon the elements of ϕ, and g represents a geometry related quantity. Then these three forms are approximated by the following second-order difference formulae:

$$\delta_\xi\left(cg\frac{\partial}{\partial\xi}s\right) \simeq \frac{(cg)_{j+1/2}(s_{j+1}-s_j)-(cg)_{j-1/2}(s_j-s_{j-1})}{\Delta\xi^2} \tag{26a}$$

$$\delta_\xi\left(cg\frac{\partial}{\partial\eta}s\right) \simeq \frac{(cg)_{j+1}(s_{j+1,k+1}-s_{j+1,k-1})-(cg)_{j-1}(s_{j-1,k+1}-s_{j-1,k-1})}{4\Delta\xi\Delta\eta} \tag{26b}$$

$$\delta_\xi(sg) \simeq \frac{(sg)_{j+1}-(sg)_{j-1}}{2\Delta\xi} \tag{26c}$$

where half-point evaluations are simply averages of the neighboring two points. Similar formulae are used for the $\delta_\eta e_v$ type terms. The operators $\Gamma_\xi^\pm$, $\Gamma_\eta^\pm$ in Eq. (24b) are one-sided difference formulae and can be either first-order or second-order, depending on the steady-state solution accuracy required. For first-order accurate steady-state solutions,

$$\Gamma_\xi^+ = \nabla_\xi,\ \Gamma_\eta^+ = \nabla_\eta,\ \Gamma_\xi^- = \Delta_\xi, \text{ and } \Gamma_\eta^- = \Delta_\eta \tag{27}$$

while achieving second-order accurate steady-state solutions requires the use of

$$\Gamma_\xi^- = \frac{1}{2}\left(3\nabla_\xi - \nabla_{\xi_{j-1}}\right) \tag{28a}$$

$$\Gamma_\eta^+ = \frac{1}{2}\left(3\nabla_\eta - \nabla_{\eta_{k-1}}\right) \tag{28b}$$

$$\Gamma_\xi^- = \frac{1}{2}\left(3\Delta_\xi - \Delta_{\xi_{j+1}}\right) \tag{28c}$$

$$\Gamma_\eta^- = \frac{1}{2}\left(3\Delta_\eta - \Delta_{\eta_{k+1}}\right) \tag{28d}$$

For example,

$$\Gamma_{\xi}^{+}\phi = \frac{1}{2}\left(3\nabla_{\xi}\phi - \nabla_{\xi}\phi_{j-1}\right), \text{ etc.}$$

In practice, the value of $\bar{\beta}$ in Eq. (24) is set to zero if the input value of β is not 1/2. This is consistent since, if $\beta = 0$ or $\beta = 1$, then the resulting algorithm is only first-order time accurate anyway, so the $\bar{\beta}$ terms are the same order as the error. Therefore, they may just as well be eliminated. If computation of the $\bar{\beta}$ terms is required, the forward time differences in Eq. (24a) may be replaced by backward time differences without compromising the accuracy of the algorithm. It is sometimes more convenient to generate differences based on past geometric information rather than future information. This is done in the present work. Note, however, that all $\bar{\beta}$ terms vanish anyway for a stationary grid.

The difference scheme represented by Eq. (24) uses fully general geometric description and is capable of handling adaptive grids. The laws governing the grid motion are not supplied but could be incorporated. The scheme can be either first- or second-order accurate in space and is currently first order in time. The addition of the viscous and source term Jacobian matrices to the left side of the difference scheme is required to produce a fully second-order accurate transient solution.

The object of the integration scheme is to produce ϕ^{n+1}. This is actually accomplished at a typical point as described in what follows. Rewrite Eq. (24a) as

$$\Omega_{\xi}\Omega_{\eta}\,\Delta\phi = \text{RHS} \tag{29}$$

where Ω_{ξ}, Ω_{η} represent the factored operators on the left side of Eq. (24a) and RHS represents everything on the right side of the equal sign. Define ϕ^{*} such that

$$\Omega_{\eta}\,\Delta\phi = \phi^{*} \tag{30}$$

Then

$$\Omega_{\xi}\,\phi^{*} = \text{RHS} \tag{31}$$

and the algorithm implementation is as follows.

1. Given ϕ at all points at level n
2. Compute RHS and elements of Ω_ξ in Eq. (31)
3. Solve block tridiagonal system to get ϕ^*
4. Compute elements of Ω_η in Eq. (30)
5. Solve Eq. (30) for $\Delta\phi$
6. Solve for $\phi^{n+1} = \phi^n + \Delta\phi$
7. Go to Step 2.

3.4 CONSERVATIVE PROPERTY

It was reported in Ref. 21 that exact satisfaction of the conservative property is essential for computation of flows with shock. (It is unclear to this author that such a requirement is strictly necessary for higher-order differencing schemes.) This requirement means that a difference scheme must numerically satisfy the following integral condition (divergence theorem)

$$\iiint_V \nabla \cdot \bar{\bar{F}}\, dV = \oiint_{\partial V} \hat{n} \cdot \bar{\bar{F}}\, dA \tag{32}$$

where $\bar{\bar{F}}$ is the flux dyadic represented in Cartesian space by $\bar{\bar{F}} = \bar{e}\hat{i} + \bar{f}\hat{j}$. For a 2-D problem in ξ, η coordinates the discrete analog of the left side of this equation is

$$\sum_j \sum_k J \nabla \cdot \bar{\bar{F}} \tag{33}$$

where $dV = Jd\xi\, d\eta$ and $d\xi$, and $d\eta$ are taken to be unity with no loss of generality. The operator $J\nabla$ is given by

$$J\nabla = \left(y_\eta \frac{\partial}{\partial \xi} - y_\xi \frac{\partial}{\partial \eta}\right)\hat{i} + \left(-x_\eta \frac{\partial}{\partial \xi} + x_\xi \frac{\partial}{\partial \eta}\right)\hat{j}$$

Therefore,

$$J\nabla \cdot \bar{\bar{F}} = y_\eta \frac{\partial \bar{e}}{\partial \xi} - y_\xi \frac{\partial \bar{e}}{\partial \eta} - x_\eta \frac{\partial \bar{f}}{\partial \xi} + x_\xi \frac{\partial \bar{f}}{\partial \eta}$$

The present flux difference splitting concept modifies this to the following

$$J\nabla \cdot \bar{\bar{F}} = Q^+\left(y_\eta \bar{e}_\xi - x_\eta \bar{f}_\xi\right) + Q^-\left(y_\eta \bar{e}_\xi - x_\eta \bar{f}_\xi\right)$$

$$+ R^+\left(x_\xi \bar{f}_\eta - y_\xi \bar{e}_\eta\right) + R^-\left(x_\xi \bar{f}_\eta - y_\xi \bar{e}_\eta\right)$$

which by substitution into Eq. (33) gives the discrete analog of the left side of Eq. (32) as

$$\sum_j \sum_k \Big[Q^+\left(y_\eta \bar{e}_\xi - x_\eta \bar{f}_\xi\right) + Q^-\left(y_\eta \bar{e}_\xi - x_\eta \bar{f}_\xi\right) \tag{34}$$

$$+ R^+\left(x_\xi \bar{f}_\eta - y_\xi \bar{e}_\eta\right) + R^-\left(x_\xi \bar{f}_\eta - y_\xi \bar{e}_\eta\right)\Big]$$

where $\sum_j \sum_k$ indicates a double summation over all points in the region of interest. Now, inspection of Eq. (32) reveals that when the double summation in Eq. (34) is expanded the result must be that all terms drop out except terms on the boundary of the domain of interest. This is simply a fact stated by the divergence theorem. However, in practice, this does not happen exactly unless special consideration is given to the evaluation of the metrics and the matrices $Q^\pm$, $R^\pm$. This special consideration, unfortunately, depends on the differencing formulae selected for $\bar{e}_\xi$, $\bar{e}_\eta$, etc. For example, consider the case of first-order spatial differences in the fluxes $\bar{e}$, $\bar{f}$. Then Eq. (34) becomes

$$\sum_j \sum_k \left(Q^+ y_\eta \nabla_\xi \bar{e} + Q^- y_\eta \Delta_\xi \bar{e} - R^+ y_\xi \nabla_\eta \bar{e} - R^- y_\xi \Delta_\eta \bar{e}\right) \tag{35}$$

$$- \sum_j \sum_k \left(Q^+ x_\eta \nabla_\xi \bar{f} + Q^- x_\eta \Delta_\xi \bar{f} - R^+ x_\xi \nabla_\eta \bar{f} - R^- x_\xi \Delta_\eta \bar{f}\right)$$

where terms involving $\bar{e}$ and $\bar{f}$ have been separated. An expansion of the double summation shows that in order to get interior point cancellation, the metrics x_ξ, x_η, y_ξ, y_η must be centrally differenced and the products $Q^+ y_\eta$, $Q^- y_\eta$, etc., are evaluated with two point

averages over the points involved with the associated finite difference. For example, to compute $Q^+y_\eta \nabla_\xi \bar{e}$, the product Q^+y_η is evaluated as

$$\left(Q^+y_\eta\right) = \frac{1}{2}\left[\left(Q^+y_\eta\right) + \left(Q^+y_\eta\right)_{j-1}\right] \tag{36}$$

This assures one of satisfying global conservation. For the case of second-order finite difference representations of the flux derivatives in Eq. (34), no method has been found of exactly satisfying the global conservation property. However if the coefficients Q^+y_η, Q^-y_η, etc., in Eq. (34) are evaluated at the point of application of the associated second-order flux difference and the summation indicated is carried out, then it can be shown using Taylor expansions that a typical interior point has a residual which reduces to

$$\frac{1}{3}\Delta\xi\Delta\eta\left(\Delta\xi^2 y_{\eta\xi\xi\xi} - \Delta\eta^2 y_{\xi\eta\eta\eta}\right) + \text{higher order terms}$$

This is consistent with the fact that the second-order difference approximations are used at each point. This error in satisying the conservative property exactly is thought to be negligible for the second-order scheme, although further tests are required to prove or disprove this hypothesis.

3.5 BOUNDARY CONDITIONS

This section describes the discretization of the boundary conditions outlined in Section 2.4. The general philosophy for all boundaries is to incorporate the boundary condition implicitly and then impose it explicitly after the integrated solution vector is determined. Refer to Fig. 5 for the following discussion. Consider applying the factored difference scheme to all interior points in the computational grid. In particular, perform the step indicated by Eq. (31) along each η (or k) = constant line excluding k = 1 and k = K. When

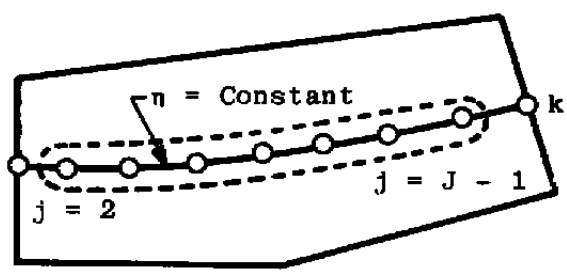

Figure 5. Typical η = constant line.

the operation indicated by Eq. (31) is expanded, the result will be a block tridiagonal system of equations to solve for ϕ^* at all points from j = 2 to j = J − 1. This system has the form

$$L_2 \phi_1^* + D_2\phi_2^* + U_2\phi_3^* = RHS_2$$

$$L_3\phi_2^* + D_3\phi_3^* + U_3\phi_4^* = RHS_3$$

$$L_{J-1}\phi_{J-2}^* + D_{J-1}\phi_{J-1}^* + U_{J-1}\phi_J^* = RHS_{J-1}$$

where L, D, and U are 4 × 4 matrix blocks representing lower, diagonal, and upper blocks, respectively. This system involves ϕ^* at j = 1 and ϕ^* at j = J. At j = 1, or boundary D of Fig. 2, the inflow data is prescribed and never changes, implying that $\Delta\phi = 0$ here. Since ϕ^* is proportional to $\Delta\phi$ as indicated by Eq. (30), then ϕ^* at j = 1 is always zero. At the j = J boundary (boundary B of Fig. 2) the value of ϕ_J^* is needed. In the present work ϕ_J^* is assumed to depend on upstream information in the following way

$$\phi_J^* \cong \alpha\phi_{J-1}^* + \beta\phi_{J-2}^* \tag{37}$$

If (α, β) are taken to be (2, −1) this is equivalent to enforcing $\phi_{\xi\xi}^* = 0$ at this boundary. $(\alpha, \beta) = (1, 0)$ implies that $\phi_\xi^* = 0$ at this boundary. Incorporation of these conditions at j = 1 and j = J results in the following system of equations.

$$\begin{bmatrix} D_2 & U_2 & 0 & 0 & 0 & & \\ L_3 & D_3 & U_3 & 0 & 0 & & \\ 0 & L_4 & D_4 & U_4 & 0 & & \\ 0 & & L_{J-3} & D_{J-3} & U_{J-3} & 0 & \\ 0 & & 0 & L_{J-2} & D_{J-2} & U_{J-2} & \\ 0 & & 0 & 0 & L_{J-1} + \beta U_{J-1} & D_{J-1} + \alpha U_{J-1} & \end{bmatrix} \begin{Bmatrix} \phi_2^* \\ \phi_3^* \\ \cdot \\ \cdot \\ \cdot \\ \cdot \\ \phi_{J-2}^* \\ \phi_{J-1}^* \end{Bmatrix} = \begin{Bmatrix} RHS_2 \\ RHS_3 \\ \cdot \\ \cdot \\ \cdot \\ \cdot \\ RHS_{J-2} \\ RHS_{J-1} \end{Bmatrix} \tag{38}$$

This block tridiagonal system is solved for ϕ_2^* through ϕ_{J-1}^* and then ϕ_J^* is computed from Eq. (37). This is repeated for each k from 2 to K − 1.

The approach just outlined for treatment of the outflow boundary is not physically correct even from a signal propagation point of view. This is because subsonic flow will always exist in the boundary layer and, technically speaking, some mechanism for upstream influence is necessary. However, the present approach does work for the class of problems considered with minimal degradation of the flow upstream of the outflow boundary.

Next, a solution to Eq. (30) for $\Delta\phi$ is required for j = 2 through J. Consider a typical ξ, j = constant line as shown in Fig. 6. Along this line, expansion of Eq. (30) yields

$$L_2\Delta\phi_1 + D_2\Delta\phi_2 + U_2\Delta\phi_3 = \phi_2^*$$

$$L_3\Delta\phi_2 + D_3\Delta\phi_3 + U_3\Delta\phi_4 = \phi_3^* \tag{39}$$

$$L_{K-1}\Delta\phi_{K-2} + D_{K-1}\Delta\phi_{K-1} + U_{K-1}\Delta\phi_K = \phi_{K-1}^* \tag{40}$$

This system involves $\Delta\phi_1$, and $\Delta\phi_K$ which are wall and upper boundary increments in the solution vector, ϕ. The treatment of $\Delta\phi_1$ is addressed first. The value of $\Delta\phi_1$ must come from the wall boundary conditions as described in Section 2.4. Since

$$\Delta\phi_1 = \left(\Delta\varrho,\ \Delta(\varrho u),\ \Delta(\varrho v),\ \Delta(\varrho e)\right)^T \tag{41}$$

from Eq. (5a), the values of each of these increments at the wall point must be determined. The no slip condition requires $\Delta(\varrho u) = \Delta(\varrho v) = 0$. The density increment, $\Delta\varrho$, is expressed in terms of temperature and pressure increments from the equation of state giving

$$\Delta\varrho = \frac{1}{RT}\Delta p - \frac{\varrho}{T}\Delta T \tag{42}$$

The normal pressure gradient condition is used to obtain

$$\Delta\left(\frac{\partial p}{\partial n}\right) = 0 = \frac{\partial}{\partial n}(\Delta p)$$

and

$$\frac{\partial}{\partial n}(\cdot) = \nabla(\cdot)\cdot\hat{n}$$

where $\hat{n} = \nabla\eta/|\nabla\eta|$ is the wall normal unit vector. So since $\nabla = \nabla\xi\,\partial/\partial\xi + \nabla\eta\,\partial/\partial\eta$,

$$(\Delta\xi \cdot \nabla\eta)\frac{\partial(\Delta p)}{\partial\xi} + (\nabla\eta \cdot \nabla\eta)\frac{\partial(\Delta p)}{\partial\eta} = 0$$

which is finite differenced to yield (see Fig. 6)

$$(\nabla\xi \cdot \nabla\eta)\left[\Delta p - \Delta p_{j-1}\right] + \frac{1}{2}(\nabla\eta \cdot \nabla\eta)\left[4\,\Delta p_2 - 3\Delta p - \Delta p_3\right] = 0 \qquad (43)$$

Note that this equation allows expression of Δp at the wall in terms of Δp at points on the interior adjacent to the wall and the first upstream wall point.

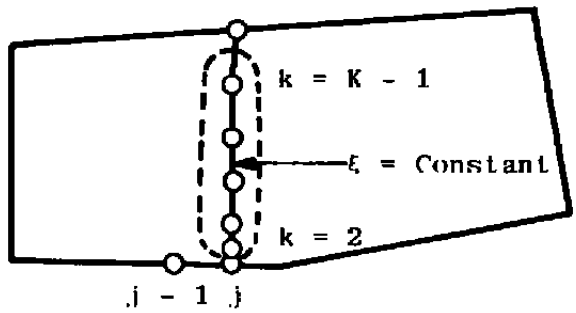

Figure 6. Typical ξ = constant line.

The temperature condition is handled as follows. Since

$$\tilde{\alpha}\frac{\partial T}{\partial n} + (1 - \tilde{\alpha})(T - T_w) = 0$$

time differencing yields

$$\tilde{\alpha}\frac{\partial}{\partial n}(\Delta T) + (1 - \tilde{\alpha})\Delta T = 0$$

and

$$\frac{\partial\Delta T}{\partial n} = \frac{\nabla\xi \cdot \nabla\eta}{|\nabla\eta|}\frac{\partial(\Delta T)}{\partial\xi} + \frac{\nabla\eta \cdot \nabla\eta}{|\nabla\eta|}\frac{\partial(\Delta T)}{\partial\eta}$$

The differenced result is

$$\tilde{\alpha}\Big[\big(\nabla\xi \cdot \nabla\eta\big)\big(\Delta T - \Delta T_{j-1}\big) + \frac{1}{2}\big(\nabla\eta \cdot \nabla\eta\big)$$

$$\big(4(\Delta T)_2 - 3(\Delta T) - (\Delta T)_3\big) - \Delta T\Big] \qquad (44)$$

$$+ \Delta T = 0$$

This equation allows expression of ΔT at the wall in terms of ΔT at points on the interior adjacent to the wall and the first upstream wall point. Recall that $\tilde{\alpha} = 0$ for a fixed wall temperature and and $\tilde{\alpha} = 1$ for an adiabatic wall condition.

The quantity $\Delta\phi_1$, in Eq. (39) must be related to the wall boundary conditions expressed by Eqs. (43) and (44) along with the no-slip condition. This is done by expressing $\Delta\phi_1$, in terms of $\Delta\phi$ at interior adjacent points and possibly $\Delta\phi$ at other selected points. First recognize that the fourth element of ϕ is total energy per unit volume expressed in terms of total energy per unit mass, e, as

$$\rho e = \frac{P}{\gamma - 1} + \frac{1}{2\rho}\Big[(\rho u)^2 + (\rho v)^2\Big]$$

A time differencing of this equation yields

$$\Delta(\rho e) = \frac{\Delta p}{\gamma - 1} - \Big(\frac{u^2 + v^2}{2}\Big)\Delta\rho + u\Delta(\rho u) + v\Delta(\rho v)$$

At the wall, due to the no-slip condition,

$$\Delta p = (\gamma - 1)\Delta(\rho e)$$

At points other than the wall, Δp is expressed in terms of the elements of $\Delta\phi$ as

$$\Delta p = (\gamma - 1)\Big[\Delta(\rho e) + \Big(\frac{u^2 + v^2}{2}\Big)\Delta\rho - u\Delta(\rho u) - v\Delta(\rho v)\Big]$$

Let the vector $\overline{m}$ be defined as

$$\overline{m} = (\gamma - 1)\left[\frac{u^2 + v^2}{2}, -u, -v, 1\right]^T \tag{45a}$$

then

$$\Delta p = \overline{m} \cdot \Delta\phi \tag{45b}$$

Further define the vector $\bar{\ell}$ as

$$\bar{\ell} = (1, 0, 0, 0)^T$$

so that

$$\Delta\varrho = \bar{\ell} \cdot \Delta\phi$$

Now from Eq. (42) it is clear that

$$\Delta T = \frac{1}{\varrho R}\Delta p - \frac{T}{\varrho}\Delta\varrho$$

or

$$\Delta T = \frac{1}{\varrho R}\overline{m} \cdot \Delta\phi - \frac{T}{\varrho}\bar{\ell} \cdot \Delta\phi$$

Let

$$\bar{n} = \frac{1}{\varrho R}\overline{m} - \frac{T}{\varrho}\bar{\ell} \tag{46a}$$

Then

$$\Delta T = \bar{n} \cdot \Delta\phi \tag{46b}$$

Substitution of Eqs. (45b) and (46b) into Eqs. (43) and (44) gives

$$\overline{am} \cdot \Delta\phi = (\nabla\xi \cdot \nabla\eta)\overline{m}_{j-1,1} \cdot \Delta\phi_{j-1,1} - 2(\nabla\eta \cdot \nabla\eta)\overline{m}_{j,2} \cdot \Delta\phi_{j,2} \tag{47}$$

$$+ \frac{1}{2}(\nabla\eta \cdot \nabla\eta)\overline{m}_{j,3} \cdot \Delta\phi_{j,3}$$

and

$$\omega\bar{n} \cdot \Delta\phi = \tilde{\alpha}(\nabla\xi \cdot \nabla\eta)\bar{n}_{j-1,1} \cdot \Delta\phi_{j-1,1} - 2\tilde{\alpha}(\nabla\eta \cdot \nabla\eta)\bar{n}_{j,2} \cdot \Delta\phi_{j,2}$$

$$+ \frac{\tilde{\alpha}}{2}(\nabla\eta \cdot \nabla\eta)\bar{n}_{j,3} \cdot \Delta\phi_{j,3} \tag{48}$$

where

$$a = (\nabla\xi \cdot \nabla\eta) - \frac{3}{2}(\nabla\eta \cdot \nabla\eta)$$

and

$$\omega = (1 - \tilde{\alpha}) + \tilde{\alpha}a$$

It is desirable to define the 4 × 4 matrices Z, X, W, Y such that the boundary condition may be expressed as

$$Z\Delta\phi_{j,1} = X\Delta\phi_{j-1,1} + W\Delta\phi_{j,2} + Y\Delta\phi_{j,3} \tag{49}$$

Equations (47) and (48) constitute the first two rows of Eq. (49) so the first two rows of the matrices Z, X, W, Y may be written down by inspection. The last two rows of Eq. (49) simply represent the no-slip condition. Let the four elements of $\bar{m}$ be represented by m_1, m_2, m_3, and m_4 and likewise for $\bar{n}$. Then the matrices Z, X, W, and Y are given by

$$Z = \begin{pmatrix} am_1 & am_2 & am_3 & am_4 \\ \omega n_1 & \omega n_2 & \omega n_3 & \omega n_4 \\ 0 & 1 & 0 & 0 \\ 0 & 0 & 1 & 0 \end{pmatrix}_{j,1} \tag{50a}$$

$$X = (\nabla\xi \bullet \nabla\eta)_{j,1} \begin{pmatrix} m_1 & m_2 & m_3 & m_4 \\ \tilde{\alpha}n_1 & \tilde{\alpha}n_2 & \tilde{\alpha}n_3 & \tilde{\alpha}n_4 \\ 0 & 0 & 0 & 0 \\ 0 & 0 & 0 & 0 \end{pmatrix}_{j-1,1} \tag{50b}$$

$$W = -2(\nabla\eta \bullet \nabla\eta)_{j,1} \begin{pmatrix} m_1 & m_2 & m_3 & m_4 \\ \tilde{\alpha}n_1 & \tilde{\alpha}n_2 & \tilde{\alpha}n_3 & \tilde{\alpha}n_4 \\ 0 & 0 & 0 & 0 \\ 0 & 0 & 0 & 0 \end{pmatrix}_{j,2} \tag{50c}$$

and

$$Y = (1/2)(\nabla\eta \bullet \nabla\eta)_{j,1} \begin{pmatrix} m_1 & m_2 & m_3 & m_4 \\ \tilde{\alpha}n_1 & \tilde{\alpha}n_2 & \tilde{\alpha}n_3 & \tilde{\alpha}n_4 \\ 0 & 0 & 0 & 0 \\ 0 & 0 & 0 & 0 \end{pmatrix}_{j,3} \tag{50d}$$

Now define $X^* = Z^{-1}X$, $W^* = Z^{-1}W$, $Y^* = Z^{-1}Y$. Then the solution increment $\Delta\phi_{j,1}$ becomes

$$\Delta\phi_{j,1} = X^*\Delta\phi_{j-1,1} + W^*\Delta\phi_{j,2} + Y^*\Delta\phi_{j,3} \tag{51}$$

Thus, with this result, Eq. (39) is modified to read

$$(D_2 + L_2W^*)\Delta\phi_2 + (U_2 + L_2Y^*)\Delta\phi_3 = \phi_2^* - L_2X^*\Delta\phi_{j-1,1} \tag{52}$$

Since the $j = 2$ ξ = constant line is computed first, the value of $\Delta\phi_{j-1,1}$ which is needed on the right-hand side of Eq. (52) is known since it falls on the inflow boundary. Each ξ = constant inversion in turn requires $\Delta\phi_{j-1,1}$ at the previously computed wall point, so as long as the sweep proceeds from left to right the quantity $\Delta\phi_{j-1,1}$ in Eq. (52) is known.

Next, the value of $\Delta\phi_K$ is needed in Eq. (40). Two approaches are considered for treating this upper boundary. The first is to consider the upper boundary one of fixed known flow properties. In this case, $\Delta\phi_K = 0$ and the block tridiagonal system of equations to solve at each ξ = constant line from $j = 2$ to $j = J$ is given by

$$\begin{pmatrix} D_2 + L_2W^* & U_2 + L_2Y^* & 0 & 0 & & & 0 \\ L_3 & D_3 & U_3 & 0 & & & 0 \\ 0 & L_4 & D_4 & U_4 & 0 & & 0 \\ 0 & & 0 & L_{K-3} & D_{K-3} & U_{K-3} & 0 \\ 0 & & & 0 & L_{K-2} & D_{K-2} & U_{K-2} \\ 0 & & & 0 & 0 & L_{K-1} & D_{K-1} \end{pmatrix} \begin{Bmatrix} \Delta\phi_2 \\ \Delta\phi_3 \\ \cdot \\ \cdot \\ \cdot \\ \Delta\phi_{K-2} \\ \Delta\phi_{K-1} \end{Bmatrix} = \begin{Bmatrix} \phi_2^* - L_2X^*\Delta\phi_{j-1,1} \\ \phi_3^* \\ \\ \\ \\ \phi_{K-2}^* \\ \phi_{K-1}^* \end{Bmatrix} \tag{53}$$

Solution of this system yields $\Delta\phi_2$ through $\Delta\phi_{K-1}$ for the given j. $\Delta\phi_K$ is zero and $\Delta\phi_1$ is computed from Eq. (51). The dependent variable, ϕ^{n+1}, is incremented giving the new solution on the given j = constant line. Due to roundoff errors, this solution will not exactly satisfy the wall boundary conditions even though these conditions are implictly satisfied. For this reason, the wall conditions are explictly enforced with the equations

$$p_{j,1} = \left[\frac{(\nabla\xi \cdot \nabla\eta)\, p_{j-1,1} + \frac{1}{2}(\nabla\eta \cdot \nabla\eta)(p_{j,3} - 4\, p_{j,2})}{(\nabla\xi \cdot \nabla\eta) - \frac{3}{2}(\nabla\eta \cdot \nabla\eta)} \right] \tag{54}$$

$$T_{j,1} = \tilde{\alpha}\left[\frac{(\nabla\xi \cdot \nabla\eta)T_{j-1,1} + \frac{1}{2}(\nabla\eta \cdot \nabla\eta)(T_{j,3} - 4\, T_{j,3})}{(\nabla\xi \cdot \nabla\eta) - \frac{3}{2}(\nabla\eta \cdot \nabla\eta)} \right] + (1 - \tilde{\alpha})T_w \tag{55}$$

$$u_{j,1} = v_{j,1} = 0 \tag{56}$$

Equations (54) - (56) provide wall information to be used to compute a new $\phi_{j,1}^{n+1}$. Even though this recomputed wall solution is only slightly different, this practice of reinforcing the wall boundary conditions explicitly will oftentimes avoid drifting in the solution.

The second approach in determining $\Delta\phi_K$ is to actually solve the governing equations on this upper boundary since, strictly speaking, the first approach of assuming $\Delta\phi_K = 0$ is physically incorrect from a signal propagation point of view. The first thing to recognize in this context is that ϕ^* must be determined at $k = K$, which requires a block tridiagonal inversion along this upper boundary. That is, Eq. (38) must be solved along $k = K$. To present a clear picture of the approach used, it is necessary to begin with the governing equations. Define the vector S such that

$$S = h_i - \xi_x \frac{\partial e_v}{\partial \xi} - \xi_y \frac{\partial f_v}{\partial \xi} - \eta_x \frac{\partial e_v}{\partial \eta} - \eta_y \frac{\partial f_v}{\partial \eta} - h_v \tag{57}$$

The governing equation is then written [see Eq. (19)] as

$$\frac{\partial \phi}{\partial \tau} + Q^+\left(\xi_t \frac{\partial \phi}{\partial \xi} + \xi_x \frac{\partial e_i}{\partial \xi} + \xi_y \frac{\partial f_i}{\partial \xi}\right) + Q^-\left(\xi_t \frac{\partial \phi}{\partial \xi} + \xi_x \frac{\partial e_i}{\partial \xi} + \xi_y \frac{\partial f_i}{\partial \xi}\right)$$

$$+ R^+\left(\eta_t \frac{\partial \phi}{\partial \eta} + \eta_x \frac{\partial e_i}{\partial \eta} + \eta_y \frac{\partial f_i}{\partial \eta}\right) + R^-\left(\eta_t \frac{\partial \phi}{\partial \eta} + \eta_x \frac{\partial e_i}{\partial \eta} + \eta_y \frac{\partial f_i}{\partial \eta}\right)$$

$$+ S = 0$$

Premultiplication of this equation by the left eigenvector matrix T_η^{-1} exposes the normalized eigenvalue matrices $\hat{\Lambda}_\eta^\pm$ on the η derivative terms. The eigenvalues associated with this direction are

$$\lambda_{1,2} = \eta_t + \eta_x u + \eta_y v = \eta_t + \bar{q} \cdot \nabla\eta$$

$$\lambda_3 = \lambda_1 + c\sqrt{\eta_x^2 + \eta_y^2}$$

$$\lambda_4 = \lambda_1 - c\sqrt{\eta_x^2 + \eta_y^2}$$

Since $\eta_t = -\bar{g} \cdot \nabla\eta$ where $\bar{g}$ is the speed vector of the point in question (important only in moving grid problems), λ_1 is expressed as

$$\lambda_1 = (\bar{q} - \bar{g}) \cdot \nabla\eta = \bar{q}_R \cdot \nabla\eta$$

where $\bar{q}_R$ represents the fluid velocity relative to the moving boundary point. It is also true that $\nabla\eta$ is a vector perpendicular to the η = constant boundary in question. In this case $\nabla\eta$ points out of the computational domain. Therefore, the sign of λ_1, indicates whether flow is into the computational domain or out of it at this η = constant boundary. If $\lambda_1 > 0$, flow exits the computational domain through the upper boundary and if $\lambda_1 < 0$ flow enters the domain through this boundary. Now consider λ_3.

$$\lambda_3 = \bar{q}_R \cdot \nabla\eta + c\sqrt{\eta_x^2 + \eta_y^2}$$

or

$$\lambda_3 = \sqrt{\eta_x^2 + \eta_y^2}\left[\bar{q}_R \cdot \hat{n} + c\right]$$

or

$$\lambda_3 = \sqrt{\eta_x^2 + \eta_y^2}\left[q_{R_N} + c\right] = c\sqrt{\eta_x^2 + \eta_y^2}(M_{R_N} + 1)$$

Likewise,

$$\lambda_4 = \sqrt{\eta_x^2 + \eta_y^2}\left[q_{R_N} - c\right] = c\sqrt{\eta_x^2 + \eta_y^2}(M_{R_N} - 1)$$

where q_{R_N} represents the relative normal velocity through the upper boundary. Note that $q_{R_N} > 0$ when flow exits the domain and $q_{R_N} < 0$ when flow enters the domain. Thus the sign on λ_3, λ_4 is determined by the relative normal Mach number at the upper boundary. For the problems considered in the present work the relative normal Mach number is a low subsonic value so that $\lambda_3 > 0$ and $\lambda_4 < 0$. In addition, the decision was made to treat the upper boundary as an outflow boundary rather than an inflow boundary. Thus $\lambda_{1,2} > 0$ which gives three positive eigenvalues and one negative eigenvalue. The compatibility equation system is

$$T_\eta^{-1}\frac{\partial \phi}{\partial \tau} + T_\eta^{-1}\left[Q^+\left(\xi_t\frac{\partial \phi}{\partial \xi} + \xi_x\frac{\partial e_i}{\partial \xi} + \xi_y\frac{\partial f_i}{\partial \xi}\right) + Q^-\left(\xi_t\frac{\partial \phi}{\partial \xi} + \xi_x\frac{\partial e_i}{\partial \xi}\right.\right.$$

$$\left.\left. + \xi_y\frac{\partial f_i}{\partial \xi}\right) + S\right] + \hat{A}_\eta^+ T_\eta^{-1}\left(\eta_t\frac{\partial \phi}{\partial \eta} + \eta_x\frac{\partial e_i}{\partial \eta} + \eta_y\frac{\partial f_i}{\partial \eta}\right) \qquad (58)$$

$$+ \hat{A}_\eta^- T_\eta^{-1}\left(\eta_t\frac{\partial \phi}{\partial \eta} + \eta_x\frac{\partial e_i}{\partial \eta} + \eta_y\frac{\partial f_i}{\partial \eta}\right) = 0$$

where on the boundary in question

$$\hat{A}_\eta^+ = \text{diag}\,(1, 1, 1, 0)$$

and

$$\hat{A}_\eta^- = \text{diag}\,(0, 0, 0, 1)$$

The η-derivatives associated with the $\hat{A}_\eta^+$ are backward difference approximations which are obtainable on the upper boundary. Therefore, consistent with $\hat{A}_\eta^+$, the first three equations of the system represented by Eq. (58) are retained. However, the fourth equation requires a forward η difference on the $\hat{A}_\eta^-$ terms which is not possible. Therefore, this fourth equation must be replaced by a boundary condition on this upper boundary. The condition chosen is to enforce a "known" static pressure. This upper boundary pressure is not really precisely known in the general case but a judicious placement of the upper boundary allows justification for the use of this condition. The result is that

$$p = \text{constant in time}$$

Thus, $p_t = 0$ and this condition must replace the fourth compatibility equation. Since

$$p = (\gamma - 1)\left[\phi_4 - \frac{\phi_2^2 + \phi_3^2}{2\phi_1}\right]$$

where ϕ_1, ϕ_2, ϕ_3, ϕ_4 are the elements of the solution vector, ϕ, p_t becomes

$$p_t = (\gamma - 1)\left[\phi_{4_t} - \frac{\phi_2}{\phi_1}\phi_{2_t} - \frac{\phi_3}{\phi_1}\phi_{3_t} + \frac{\phi_2^2 + \phi_3^2}{2\phi_1^2}\phi_{1_t}\right]$$

or $p_t = \overline{m} \cdot \phi_t$ where $\overline{m}$ is defined by Eq. (45a). Since $p_t = p_\tau + \xi_t p_\xi + \eta_t p_\eta$ the pressure condition is expressed as

$$\overline{m} \cdot \phi_\tau + \xi_t \overline{m} \cdot \phi_\xi + \eta_t \overline{m} \cdot \phi_\eta = 0 \tag{59}$$

Equation (59) must replace the fourth compatibility equation of the system represented by Eq. (58). This is accomplished by first defining a nonsingular 4×4 matrix D^{-1}, which has the first three rows identical to T_η^{-1}. The last row of D^{-1} is the vector $\overline{m}$. Also let $T_{\eta *}^{-1}$ represent T_η^{-1} with the last row replaced by zeros. With these definitions, Eqs. (58) and (59) are expressed as

$$D^{-1}\phi_\tau + D^{-1}Q^+\xi_t\phi_\xi + D^{-1}Q^-\xi_t\phi_\xi + D^{-1}\eta_t\phi_\eta$$

$$+ T_\eta^{-1*}\left[Q^+\left(\xi_x\frac{\partial e_i}{\partial \xi} + \xi_y\frac{\partial f_i}{\partial \xi}\right) + Q^-\left(\xi_x\frac{\partial e_i}{\partial \xi} + \xi_y\frac{\partial f_i}{\partial \xi}\right) + S\right.$$

$$\left. + \left(\eta_x\frac{\partial e_i}{\partial \eta} + \eta_y\frac{\partial f_i}{\partial \eta}\right)\right] = 0$$

where all η derivatives are backward in sense. Premultiplication by D yields

$$\phi_\tau = -\left\{Q^+\xi_t\phi_\xi + Q^-\xi_t\phi_\xi + \eta_t\phi_\eta + DT_{\eta *}^{-1}\left[\left(\eta_x\frac{\partial e_i}{\partial \eta} + \eta_y\frac{\partial f_i}{\partial \eta}\right) + S\right.\right.$$

$$\left.\left. + Q^+\left(\xi_x\frac{\partial e_i}{\partial \xi} + \xi_y\frac{\partial f_i}{\partial \xi}\right) + Q^-\left(\xi_x\frac{\partial e_i}{\partial \xi} + \xi_y\frac{\partial f_i}{\partial \xi}\right)\right]\right\} \tag{60}$$

which is expressed in factored finite difference form as

$$\left\{I + \beta\Delta\tau\left[Q^+\,\xi_t\,\nabla_\xi I + DT_{\eta *}^{-1}\,Q^+\left(\xi_x\nabla_\xi A + \xi_y\nabla_\xi B\right)\right]\right.$$

$$\left. + \beta\Delta\tau\left[Q^-\xi_t\Delta_\xi I + DT_{\eta *}^{-1}\,Q^-\left(\xi_x\Delta_\xi A + \xi_y\Delta_\xi B\right)\right]\right\} \times$$

$$\left\{I + \beta\Delta\tau\left[\eta_t\nabla_\eta I + DT_{\eta *}^{-1}\left(\eta_x\nabla_\eta A + \eta_y\nabla_\eta B\right)\right]\right\}\Delta\phi = \Delta\tau\phi_\tau$$

$$- \bar{\beta}\Delta\tau\Big[Q^{+}\Delta\xi_t\nabla_\xi\phi + DT_{\eta^*}^{-1}\, Q^{+}\Big(\Delta\xi_x\nabla_\xi e_i + \Delta\xi_y\nabla_\xi f_i\Big)$$

$$+ Q^{-}\Delta\xi_t\Delta_\xi\phi + DT_{\eta^*}^{-1}\, Q^{-}\Big(\Delta\xi_x\Delta_\xi e_i + \Delta\xi_y\Delta_\xi f_i\Big) \qquad (61)$$

$$+ \Delta\eta_t\nabla_\eta\phi + DT_{\eta^*}^{-1}\Big(\Delta\eta_x\nabla_\eta e_i + \Delta\eta_y\nabla_\eta f_i\Big)\Big]$$

$$+ \bar{\beta}\Delta\tau\Big(\Delta\xi_x\delta_\xi e_v + \Delta\xi_y\delta_\xi f_v + \Delta\eta_x\delta_\eta e_v + \Delta\eta_y\delta_\eta f_v\Big)$$

where the same approximations used in arriving at Eq. (24a) for interior points were used here. In practice, the viscous terms in Eq. (61) are not included since they are expected to be negligible at the upper boundary. Equation (61) may be expressed as

$$\Omega_\xi\Omega_\eta\Delta\phi = \text{RHS}$$

or

$$\Omega_\xi\phi^* = \text{RHS}$$

This latter form is used to compute ϕ^* along the k = K, η = constant boundary as indicated for other η = constant lines. Then since the operator Ω_η is one-sided, the block tridiagonal system to solve for $\Delta\phi$ along each ξ = constant line is written by appending the boundary equation to the system expressed by Eq. (53) yielding

$$\begin{bmatrix} D_2 + L_2W^* & U_2 + L_2Y^* & 0 & 0 & & & \\ L_3 & D_3 & U_3 & 0 & & & \\ 0 & L_4 & D_4 & U_4 & & & \\ & & \ddots & \ddots & \ddots & & \\ & & L_{K-2} & D_{K-2} & U_{K-2} & 0 & \\ & & 0 & L_{K-1} & D_{K-1} & U_{K-1} & \\ & & 0 & 0 & L_K & D_K & \end{bmatrix} \begin{Bmatrix} \Delta\phi_2 \\ \Delta\phi_3 \\ \vdots \\ \Delta\phi_{K-1} \\ \Delta\phi_K \end{Bmatrix} = \begin{Bmatrix} \phi_2^* - L_2X^*\Delta\phi_{j-1,1} \\ \phi_3^* \\ \vdots \\ \phi_{K-1}^* \\ \phi_K^* \end{Bmatrix}$$

This system is solved for $\Delta\phi_2$ through $\Delta\phi_K$ for each ξ = constant line beginning with j = 2 and ending with j = J. The wall point is updated as discussed. The vector ϕ_K is modified to assure satisfaction of the implicitly enforced pressure condition. This is done by simply accepting the first three elements of ϕ_K and recomputing the fourth element using the correct pressure value. If this step is not performed it is possible for the upper boundary pressure to deviate from its desired value due to round off error. This is particularly true when a large number of integration steps is taken.

3.6 INITIAL CONDITIONS

Before the governing equations are integrated using the techniques described in the present work, the computational domain must be initialized to some starting solution. For the class of problems considered, this starting solution is somewhat arbitrary since only the steady-state solution is of interest. It is first assumed that the solution on the inflow boundary is known by some means. This could be data supplied by another computer code, for example. Then the solution on each ξ = constant line, in turn, is set equal to the solution on the upper boundary. This procedure is simple and reliable for the class of problems considered.

4.0 APPLICATIONS

Two computer codes were written using the procedures outlined. The first is called VISCODE and the second is VISCOD2. VISCODE imposes a fixed boundary condition in all dependent variables on the upper boundary of the computational domain. VISCODE2 imposes a fixed condition only on static pressure, and the remaining variables are computed on the upper boundary. VISCODE was applied to a Couette flow problem and VISCOD2 was applied to a flat plate laminar boundary-layer problem.

4.1 COUETTE FLOW

Figure 7 depicts a schematic of a Couette flow problem. The problem tested was characterized by the following parameters: U_∞ = 100 meters per sec, $p_\infty = 10^5$ Newtons per square meter, T_∞ = 290.36 °K, and y_{max} = 4 m. A coarse 5 × 5 grid was used to solve this problem. This problem has an exact solution when coefficients of viscosity and thermal conductivity are constant. The exact solutions for velocity and temperature distributions are given by

$$u(y) = U_\infty\left(\frac{y}{y_{max}}\right)$$

$$T(y) = \left(1 - \frac{y}{y_{max}}\right)T_w + \left(\frac{y}{y_{max}}\right)T_\infty + \frac{\mu}{2k}U_\infty^2\left(\frac{y}{y_{max}}\right)\left(1 - \frac{y}{y_{max}}\right)$$

for a fixed wall temperature, T_w, and

$$T(y) = T_\infty + \frac{\mu}{2k} U_\infty^2 \left[1 - \left(\frac{y}{y_{max}} \right)^2 \right]$$

for an adiabatic wall. Figures 8 through 10 illustrate a comparison of the numerical solution versus the exact solution for temperature profiles in a fixed wall temperature environment. The three fixed wall temperatures tested were $T_w = 0.5\ T_\infty$, $T_w = T_\infty$, and $T_w = 2T_\infty$. Figure 11 depicts the temperature profile comparison for the adiabatic wall case. Figure 12 illustrates the velocity profile comparison.

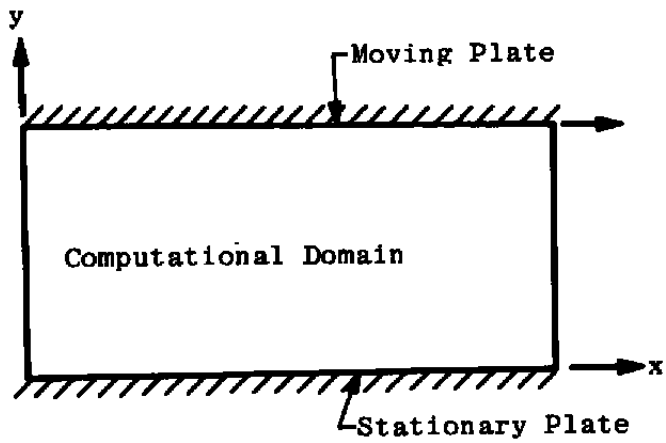

Figure 7. Couette flow schematic.

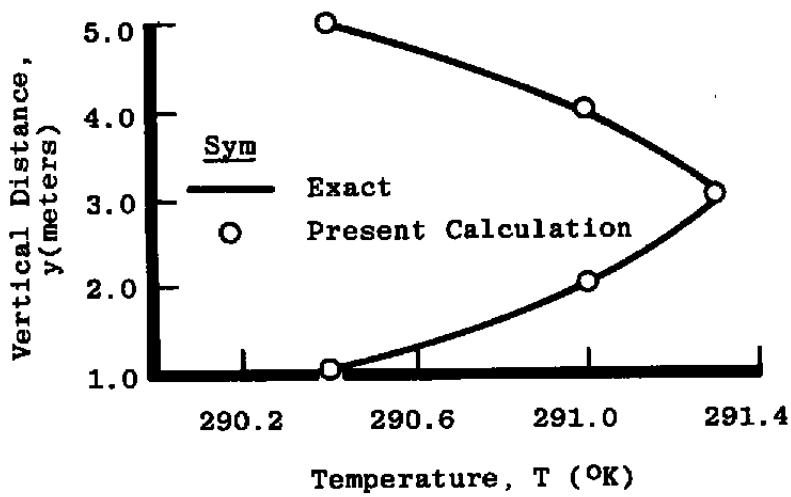

Figure 8. Temperature profile, $T_w = T_\infty$

This test problem was chosen as the first step in the code validation process. As Figs. 8 - 12 illustrate, the numerical solution is right on target for this problem.

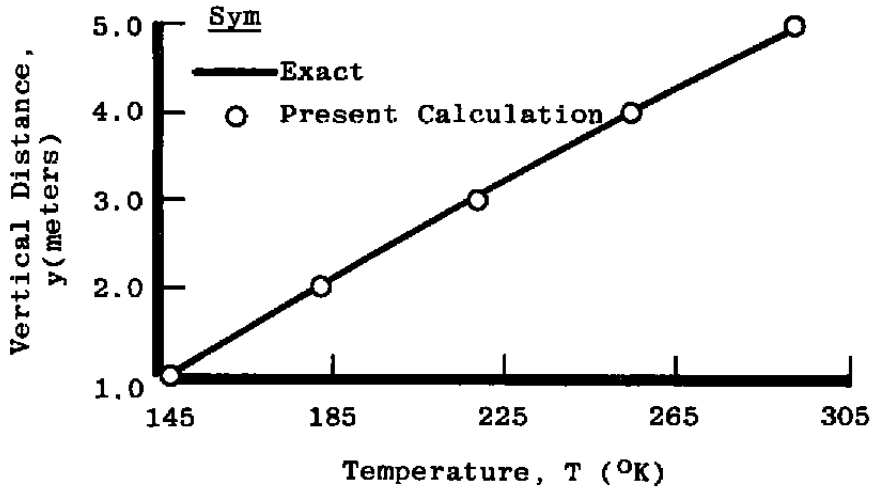

Figure 9. Temperature profile, $T_w = 0.5\ T_\infty$.

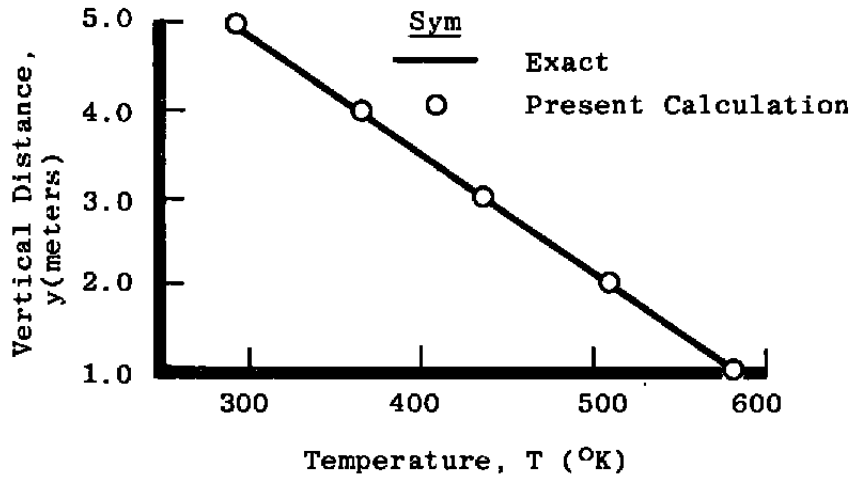

Figure 10. Temperature profile, $T_w = 2\ T_\infty$.

4.2 BLASIUS FLAT PLATE BOUNDARY LAYER

An incompressible laminar boundary layer on a flat plate was chosen as the second code validation case. See Fig. 13 for a schematic. This problem has an "exact" solution formulated in terms of a solution to a third-order ordinary differential equation. This Blasius solution is well known and provides an additional comparison case against the

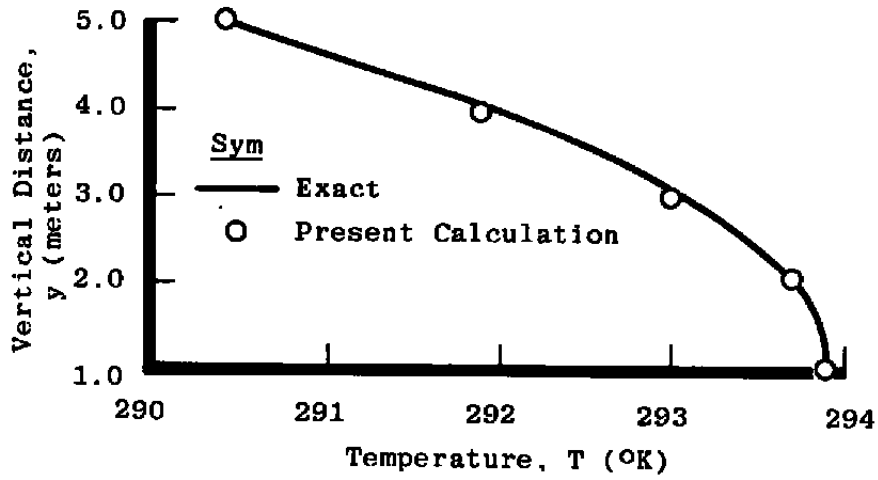

Figure 11. Temperature profile, adiabatic wall.

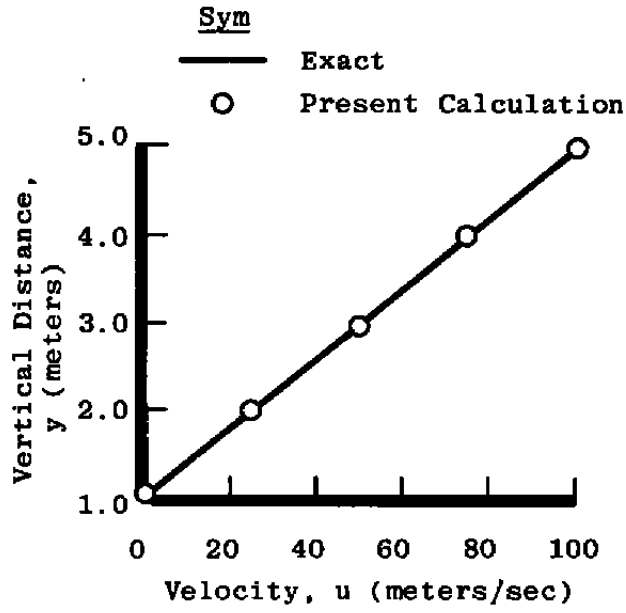

Figure 12. Representative velocity profile.

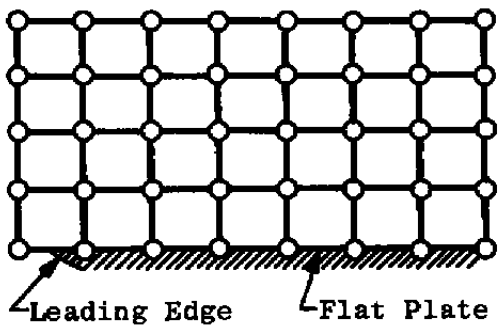

Figure 13. Flat plate problem schematic.

numerical solution. VISCOD2 was used to compute the numerical solutions. Even though the exact solution used is for an incompressible flow, the solution to the compressible equations should compare favorably if the test case Mach number is sufficiently small. The test case chosen is characterized by the following parameters: $R_{e_L} = 10^5$, $U_\infty = 100$ ft/sec, $T_\infty = 500$ °R, and $P_r = 1$ where R_{e_L} is the Reynolds number based on the length of the flat plate and P_r is the Prandtl number. The plate wall temperature is fixed at 600°R. These conditions translate to a Mach number of 0.09, which is sufficiently small to justify the comparison. The exact solution for the temperature profile as a function of local velocity for the problem described is given by

$$T(u) = \left(1 - \frac{u}{U_\infty}\right)T_w + \left(\frac{u}{U_\infty}\right)T_\infty + \frac{uU_\infty}{2c_P}\left(1 - \frac{u}{U_\infty}\right)$$

where c_p is the specific heat at constant pressure of air.

A comparison of known versus numerical solutions is found in Figs. 14 and 15. Figure 14 depicts the velocity profile comparison at a downstream station. Two numerical solutions are presented in this figure. One is for the case of a uniformly spaced grid in the y-direction and the other is for the case of a grid clustered toward the plate to the extent that the first point off the wall is at y = 0.0005 ft. In both cases, 30 points in the y direction were used. Figure 15 illustrates the comparison for the boundary-layer temperature profile at a downstream station. All comparisons show good agreement. As a result, this part of the code validation is considered to be successful.

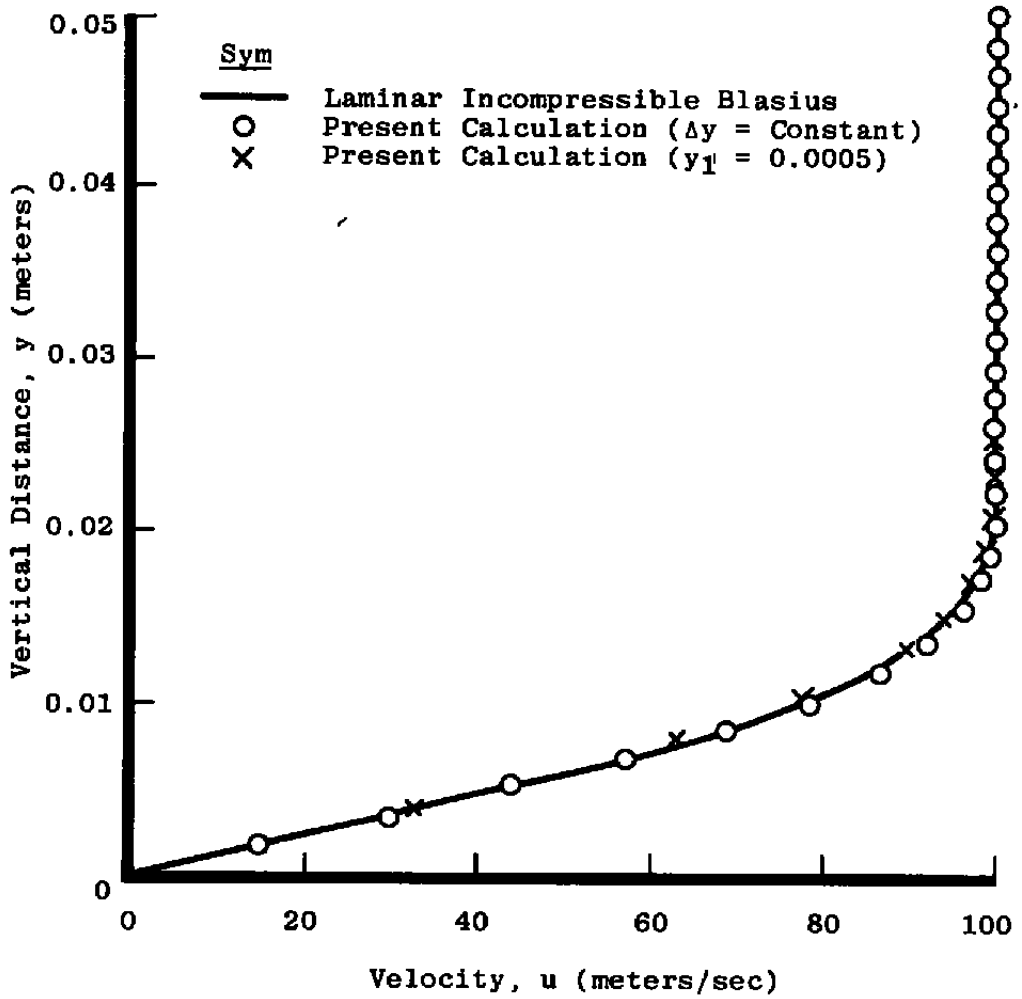

Figure 14. Velocity profile at exit plane.

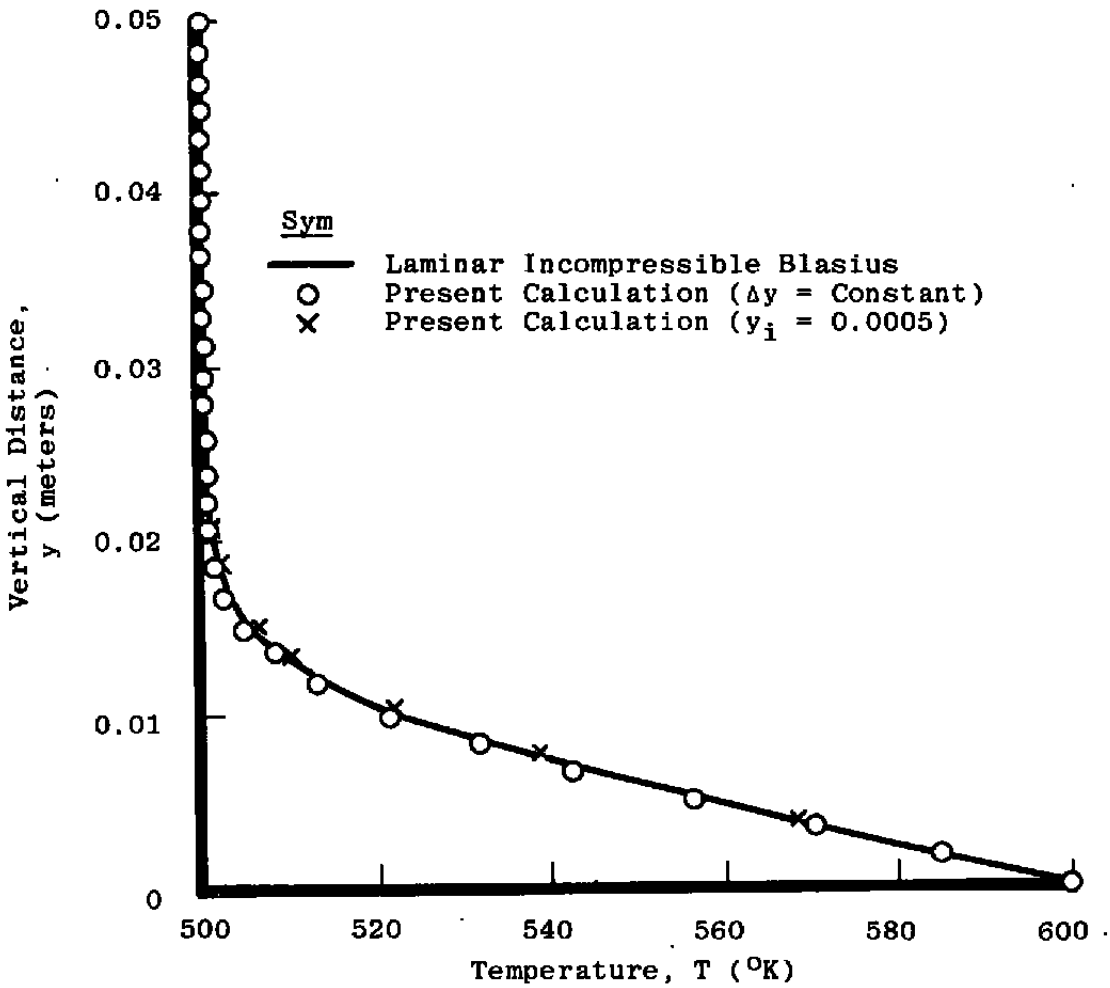

Figure 15. Temperature profile at exit plane.

5.0 CONCLUSIONS AND FUTURE WORK

A two-dimensional or axisymmetric Navier-Stokes code was developed. The code is formulated using a factored delta form. All inviscid terms are treated using a flux difference splitting concept. The viscous terms are centrally differenced. A fully general geometric description is employed and all metric terms are retained, including those pertaining to a moving grid. The algorithm as presently constructed is first order in time and either first or second order in space. It can be made seond order in time by the inclusion of the viscous and source term Jacobians in the operators on the factored side of the scheme. The code shows very promising stability properties and convergence rate. Two codes were actually developed. One imposes a fixed strategy for all variables on the upper boundary of the computational domain. The other imposes a fixed strategy only on the static pressure at this upper boundary. Validation runs were made on a Couette flow problem and a Blasius flat plate boundary layer. Results were good. The code must yet be validated on axisymmetric problems and problems with shocks such as a simple ramp induced shock-boundary layer interaction. A turbulence model is currently being incorporated to extend the current capability to turbulent flows. Future work should also include a conclusive study of the importance of the conservative property and possibly development of an adaptive grid scheme for the class of problems of interest.

REFERENCES

1. Hung, C. M. and MacCormack, R. W. "Numerical Solutions of Supersonic and Hypersonic Laminar Flows Over a Two-Dimensional Compression Corner." AIAA Paper No. 75-2, AIAA 13th Aerospace Sciences Meeting, Pasadena, California, January 1975.

2. MacCormack, Robert W. "An Efficient Numerical Method for Solving the Time-Dependent Compressible Navier-Stokes Equations at High Reynolds Numbers." NASA TMX-73,129, July 1976.

3. Shang, J. S. and Hankey, W. L., Jr. "Numerical Solution of the Navier-Stokes Equations for Supersonic Turbulent Flow Over A Compression Ramp." AIAA Paper No. 75-3, AIAA 13th Aerospace Sciences Meeting, Pasadena, California, January 1975.

4. Carter, J. E. "Numerical Solutions of the Navier-Stokes Equations for the Supersonic Laminar Flow Over a Two-Dimensional Compression Corner." NASA TR R-385, July 1972.

5. Hindman, Richard G., "Modifications to MacCormack's 2-D Navier-Stokes Compression Ramp Code for Application to Flows with Axes of Symmetry and Wall Mass Transfer." AEDC-TR-80-24 (AD-A093742), January 1981.

6. Settles, Gary S., Vas, Irwin E., and Bogdonoff, Seymour M. "Shock Wave-Turbulent Boundary Layer Interaction at a High Reynolds Number, Including Separation and Flowfield Measurements." AIAA Paper No. 76-164, AIAA 14th Aerospace Sciences Meeting, Washington, D. C., January 1976.

7. Middlecoff, J. F. and Thomas, P. D. "Direct Control of the Grid Point Distribution in Meshes Generated by Elliptic Equations." AIAA Paper 79-1462, AIAA Computational Fluid Dynamics Conference, Williamsburg, Virginia, July 23-25, 1979.

8. Winslow, A. "Numerical Solution of the Quasilinear Poisson Equation." *Journal of Computational Physics*, Vol. 1, 1966, pp. 149 - 172.

9. Thompson, J. F., Thames, F. C., and Mastin, C. M. "Automatic Numerical Generation of Body-Fitted Curvilinear Coordinate System for Field Containing Any Number of Arbitrary Two-Dimensional Bodies." *Journal of Computational Physics*, Vol. 15, 1974, pp. 299 - 319.

10. Roberts, G. O. "Computational Meshes for Boundary Layer Problems." *Lecture Notes in Physcis*, Springer-Verlag, New York, 1971, pp. 171 - 177.

11. Courant, R., Isaacson, E., and Rees, M. "On the Solution of Nonlinear Hyperbolic Differential Equations by Finite-Differences." *Communications on Pure and Applied Mathematics*, Vol. 5, 1952, pp. 243 - 255.

12. Gordon, P. "The Diagonal Form of Quasi-Linear Hyperbolic Systems as a Basis for Difference Equations." General Electric Company, Final Report, Naval Ordnance Laboratory Contract No. N60921-7164, December 1969, pp. II.D-1, II.D-22.

13. Scala, S. M. and Gordon P. "Solution of the Time-Dependent Navier-Stokes Equations for the Flow of Dissociating Gas over a Circular Cylinder." *Fluid Physics of Hypersonic Wakes*, Proceedings of AGARD, NATO Conference, Fort Collins, Colorado, May 10 - 12, 1967.

14. Moretti, G. "An Old Integration Scheme for Compressible Flows Revisted, Refurbished, and Put to Work." Polytechnic Institute of New York, POLY M/AE Report No. 78-22, September 1978.

15. Moretti, G. "The λ-Scheme." *Computers and Fluids*, Vol. 7, 1979, pp. 191 - 205.

16. Steger, J. L., and Warming, R. F. "Flux Vector Splitting of the Inviscid Gasdynamic Equations with Applications to Finite Difference Methods." *Journal of Computational Physics*, Vol. 40, April 1981, pp. 263 - 293.

17. Chakravarthy, S. R., Anderson, D. A., and Salas, M. D. "The Split Coefficient Matrix Method for Hyperbolic Systems of Gasdynamic Equations." AIAA Paper 80-0268, Pasadena, California, 1980.

18. Lombard, C. K., Oliger, J. and Yang, J. Y. "A Natural Conservative Flux Difference Splitting for the Hyperbolic Systems of Gasdynamics." AIAA Paper 82-0976, 1982.

19. Yang, Jaw-Yen, Lombard, C. K., and Bershader, D. "A Characteristic Flux Difference Splitting for the Hyperbolic Conservation Laws of Inviscid Gasdynamics." AIAA Paper 83-0040, Reno, Nevada, January 1983.

20. Lax, P. D. "Weak Solutions for Nonlinear Hyperbolic Equations and Their Numerical Computation." *Communications on Pure and Applied Mathematics*, Vol. 7, February 1954, pp. 159 - 193.

21. Warming, R. F., and Beam, R. M. "Upwind Second-Order Difference Schemes and Applications in Aerodynamic Flows." *AIAA Journal*, Vol. 14, September 1976, pp. 1241 - 1249.

NOMENCLATURE

A	Jacobian matrix associated with x-direction inviscid flux
a	Coefficient used in application of wall boundary condition
A*	Jacobian matrix associated with ξ-direction inviscid flux
B	Jacobian matrix associated with y-direction inviscid flux
B*	Jacobian matrix associated with η-direction inviscid flux
C	Jacobian matrix associated with x-direction viscous flux

c	Sonic velocity Also a solution dependent coefficient used to explain viscous term differencing
c_p	Specific heat at constant pressure
D	Jacobian matrix associated with y-direction viscous flux Also diagonal matrix in block tri-diagonal system Also inverse of boundary condition altered matrix of left eigenvectors
D^{-1}	Boundary condition altered matrix of left eigenvectors
e	Specific total energy Also y-direction flux vector in cylindrical frame
$\bar{e}$	y-direction flux vector in Cartesian frame
e_i	Inviscid part of y-direction flux vector in cylindrical frame
$\bar{e}_i$	Inviscid part of y-direction flux vector in Cartesian frame
e_v	Viscous part of y-direction flux vector in cylindrical frame
$\bar{e}_v$	Viscous part of y-direction flux vector in Cartesian frame
$\bar{\bar{F}}$	Dyadic flux function for Navier-Stokes equations
f	x-direction flux vector in cylindrical frame
$\bar{f}$	x-direction flux vector in Cartesian frame
f_i	Inviscid part of x-direction flux vector in cylindrical frame
$\bar{f}_i$	Inviscid part of x-direction flux vector in Cartesian frame
f_v	Viscous part of x-direction flux vector in cylindrical frame
$\bar{f}_v$	Viscous part of x-direction flux vector in Cartesian frame
G	Grid clustering function

g	Geometry related coefficient used to explain viscous term differencing
$\bar{g}$	Grid point speed vector
h	Source term in cylindrical frame
H_i	Jacobian matrix associated with inviscid source
h_i	Inviscid part of source term in cyindrical frame
H_v	Jacobian matrix associated with viscous source
h_v	Viscous part of source term in cylindrical frame
I	Identity matrix
$\hat{i}$	x-direction unit vector
J	Jacobian of coordinate transformation Also number of grid points in the ξ-direction
j	ξ-direction index
$\hat{j}$	y-direction unit vector
K	Number of grid points in the η-direction
k	Coefficient of thermal conductivity Also η-direction index
L	Lower off-diagonal matrix in block tri-diagonal system
$\bar{\ell}$	Vector used in application of body boundary condition
$\bar{m}$	Vector used in application of body boundary condition
M_{R_N}	Relative normal Mach number used at upper boundary
n	Direction normal to a surface Unit vector in direction of n

$\bar{n}$	Vector used in application of body boundary condition
P	ξ-forcing function in grid generation scheme
p	Static pressure
Pr	Prandtl Number
Q	η-forcing function in grid generation scheme
q	Cylindrical velocity vector
$\bar{q}$	Cartesian velocity vector
$\bar{q}_R$	Relative velocity vector
q_{R_N}	Relative normal velocity
$Q^{\pm}$	Rotation matrices used to control differencing of ξ-direction inviscid terms
R	Gas constant
$\bar{r}$	Position vector
$R^{\pm}$	Rotation matrices used to control differencing of η-direction inviscid terms
RHS	Right hand side of integration algorithm
S	Solution dependent quantity used to explain viscous term differencing; total arc length along ζ = constant curve; also represents grouping of source and viscous terms
s	Arc length along grid lines
T	Temperature
t	Time
T_ξ	Matrix of right eigenvectors associated with ξ-direction
T_ξ^{-1}	Matrix of left eigenvectors associated with ξ-direction

T_η	Matrix of right eigenvectors associated with η-direction
T_η^{-1}	Matrix of left eigenvectors associated with η-direction
U	Upper off-diagonal matrix in block tri-diagonal system
u	x-direction cylindrical velocity
$\bar{u}$	x-direction Cartesian velocity
U_∞	Free-stream velocity
v	y-direction cylindrical velocity
$\bar{v}$	y-direction Cartesian velocity
W	Matrix used in application of body boundary conditions
W*	Matrix used in application of body boundary conditions
X	Matrix used in application of body boundary conditions
x	Independent Cartesian coordinate
X*	Matrix used in application of body boundary conditions
Y	Matrix used in application of body boundary conditions
y	Independent Cartesian coordinate
Y*	Matrix used in application of body boundary conditions
Z	Matrix used in application of body boundary conditions
z	Independent Cartesian coordinate
α	Coefficient used in grid equations
	Also used in extrapolated outflow boundary condition

$\tilde{\alpha}$	Used as switch to choose temperature boundary condition
β	Coefficient used in grid generation Also a parameter used in clustering the grid Also used in extrapolated outflow boundary condition Also used to switch order of time differencing
$\bar{\beta}$	Related to β as used to switch order of time differencing
Γ^+	General backward difference operator
Γ^-	General forward difference operator
γ	Coefficient used in grid generation Also ratio of specific heats
Δ, ∇	Forward and backward difference respectively
δ	Half point central difference operator
ζ	Transformed independent variable
η	Transformed independent variable
$\bar{\eta}$	Normalized transformed independent variable
Λ	Diagonal eigenvalue matrix
Λ^+	Diagonal eigenvalue matrix of positive eigenvalues
Λ^-	Diagonal eigenvalue matrix of negative eigenvalues
$\Lambda^\pm$	Normalized diagonal eigenvalue matrix with positive or negative elements
λ	Second coefficient of viscosity Also eigenvalue of Jacobian matrix
μ	First coefficient of viscosity
ξ	Transformed independent variable

ϱ	Fluid density
Σ	Indicates discrete summation Also used in extrapolated outflow boundary condition
τ	Temporal coordinate
Φ	A part of forcing function used in grid generation
ϕ	Cylindrical dependent variable vector
$\bar{\phi}$	Cartesian dependent variable vector
ϕ^*	Intermediate dependent variable vector
ψ	A part of forcing function used in grid generation
Ω_ξ	η-direction factored implicit operator
Ω_η	η-direction factored implicit operator
ω	Coefficient used in application of wall boundary condition

Subscripts

i	Inviscid
j,k	Grid point indices
t,x,y,τ,ξ,η	Indicates partial differentiation in associated direction Also indicates simple association with a particular direction
v	Viscous
w	Wall

Superscripts

n	Temporal index
T	Transpose
+	Associated with positive eigenvalues
-	Associated with negative eigenvalues

Other

∇	Gradient operator Also backward finite difference
∇^2	Laplacian operator